EFFECT OF TOPOGRAPHY IN SATELLITE RAINFALL ESTIMATION ERRORS: OBSERVATIONAL EVIDENCE ACROSS CONTRASTING ELEVATION IN THE BLUE NILE BASIN

M.Sc.Thesis

By:

GEBREHIWOT NIGUSE TESFAY

ETHIOPIAN INSTITUTE OF WATER RESOURCES

ADDIS ABABA UNIVERSITY

ETHIOPIA

MAY, 2013

Gebrehiwot Niguse;
MSc Candidate

"BUILDING ETHIOPIA'S WATER FUTURE TOGETHER"

Ethiopian Institute of Water Resources
P.O.Box 150461, Addis Ababa, Ethiopia
T +251-11-4341698
F +251-11-1239 480
E info@eiwr.org
I www.eiwr.org

Addis Ababa University
P.O.Box:1176, Addis Ababa, Ethiopia
T +251-11-1239 768
F +251-11-1239 752
I www.aau.edu.et

MSc Thesis on:

Effect of Topography in Satellite Rainfall Estimation Errors: Observational Evidence across Contrasting Elevation in the Blue Nile Basin

By:

Gebrehiwot Niguse Tesfay

gebnig@gmail.com /gebrehiwot.tesfaye@uconn.edu

Supervised By:

Dr. Mekonnen Gebremichael: University of Connecticut, USA

Dr. Menberu Meles Bitew: University of Connecticut, USA

ADDIS ABABA UNIVERSITY

ETHIOPIA

MAY, 2013

ADDIS ABABA UNIVERSITY

Effect of Topography in Satellite Rainfall Estimation Errors: Observational Evidence across Contrasting Elevation in the Blue Nile Basin

Thesis Submitted to Ethiopian Institute of Water Resources in Partial Fulfilment of the Requirements for the Degree of Master of Science

In

Water Resources Engineering and Management

(Specialization: Surface Water Engineering and Management)

By: Gebrehiwot Niguse Tesfay

APPROVED BY BOARD OF EXAMINERS

Dr. Mekonnen Gebremichael	----------	06/19/2013
(Supervisor)	*Signature*	*Date*
Dr. Menberu Meles Bitew	----------	06/18/2013
(Co-Supervisor)	*Signature*	*Date*
Dr. Dereje Hailu	----------	----------
(External Examiner)	*Signature*	*Date*
Dr. Yilma Seleshi	----------	----------
(Internal Examiner)	*Signature*	*Date*
Ms. Adanech Yared (MSc.)	----------	----------
(Chairman)	*Signature*	*Date*

STATEMENT OF AUTHOR

I, Gebrehiwot Niguse Tesfay, declare that this thesis is my work and that all sources of materials used for this thesis have been duly acknowledged. Further, I declare that when research paper is published from the thesis following sentence will appear at the bottom of the first page of the article or at the end of the article.

Name: ..... Signature: ..... Date: .....

BIOGRAPHICAL SKETCH

The Author, Gebrehiwot Niguse Tesfay, was born on Oct. 05, 1985 G.C in Adwa Woreda, Tigray Regional State, Ethiopia. He started his schooling in 1993 G.C in Bete-yohannes elementary school, Adwa. He completed his secondary school in Nigste-Saba Comprehensive Secondary School in 2004, Adwa. And then, he joined to Hawassa University to attend a Bachelor of Science degree in Agricultural Engineering and Mechanization. After his graduation in July, 2008, he immediately recruited in the same university as a graduate assistant. Gebrehiwot joined in June 2011 to the Master of Science degree program of Water Resources Engineering and Management (specialization: Surface Water Hydrology) in Ethiopian Institute of Water Resources at Addis Ababa University, Ethiopia.

ACKNOWLEDGEMENT

I would like to express my deepest gratitude to my advisors, Dr. Mekonnen Gebremichael and Dr. Menberu Meles Bitew for their priceless support in supervising my work and providing their invaluable guidance, constructive comments and encouragement. On top of this, Dr. Menberu did field tour during instrument setup and provided us remarkable technical supports.

At this point, I am happy to thank Mr. Feyera Hirpa, who helped me in processing different formats of remotely sensed sources rainfall data in to meaningful information.

I would like to extend my gratitude to the American people for the financial support through the United State Agency for International Development (USAID) through the Higher Education for Development (HED) funded grant in the Africa-US Higher Education Initiative - HED052-9740-ETH-11-01.

My sincere appreciation goes to all staff members of Ethiopian Institute of Water Resource (EIWR) for their actively facilitating all required activities for the field work. I also appreciate their effort in preparation of seminars from Water and Environment sectors.

I will take this opportunity to thank my colleagues in the Blue Nile team, Shambel Habte and Nebiyu Solomon (EIWR MSc candidates) for their good field work cooperation.

My sincere appreciation also goes to Guba Woreda administration for remarkable cooperation during the field campaign. They assigned field guider who assisted and introduced me with the landowners in language translation, guiding us on possible location in the area and informing the objective of the work to the residents.

I would like also thank Mr. Yihdego Tesfay and all my friends who helped me directly or indirectly, in carrying out my research through remarkable encouragement, advice, and collaboration in every aspect.

Finally, but not least, my special acknowledgment goes to all my families for their help in various ways.

LIST OF ABBREVIATION AND ACRONYMS

AMSR-E = Advanced Microwave Scanning Radiometer for the Earth Orbiting System

CMORPH = Climate prediction center MORPHing technique

DEM = Digital Elevation Model

FTP = File Transfer Protocol

GPS = Global Positioning System

HDF = Hierarchical Data Format

IDL = Interactive Data Language

ITCZ = Inter-Tropical Convergence Zone

m asl = meter above sea level

NASA = National Atmospheric and ocean Administration

NOAA = National Oceanic and Atmospheric Administration

PERSIANN-CCS = Precipitation Estimation from Remotely Sensed Information using Artifical Neural Networks – Cloud Classification System

RDam = Renaissance Dam

TMPA-RT = TRMM Multi-satellite Precipitation Analysis- near Real Time

TMPA-V7 = TRMM Multi-satellite Precipitation Analysis- Version7

TRMM = Tropical Rainfall Measuring Mission

UTC = Coordinated Universal Time

WGS84 = World Geodetic System 1984; datum used by GPS

LIST OF TABLES

LIST OF FIGURES

LIST OF APPENDICES

Appendix II: Figure

Appendix II: Table

TABLE OF CONTENTS

Effect of Topography in Satellite Rainfall Estimation Errors: Observational Evidence across Contrasting Elevation in the Blue Nile Basin

ABSTRACT

In this study, the effect of topography on spatial and temporal variability of rainfall on local (25 km by 25 km grid) scale was analyzed across two contrasting elevation locations. We deployed 10 in high elevation grid (average elevation 2097m) and 9 tipping rain gauges in low elevation grid (average elevation= 695 m). Based on high quality data from the dense rain gauges, we evaluated the spatio-temporal properties of rainfall and evaluated the errors in widely used high resolution satellite rainfall estimates. Three satellite rainfall estimates; TMPA 3B42RT, TMPA 3B42V7 and CMORPH were evaluated using statistical and categorical verification measures. Our results showed that there is significantly large spatio-temporal variability of rainfall at local scale. Diurnal cycle also indicated that, low elevation receives more rainfall at early morning and the high elevation gets more rainfall between the afternoon and mid-night. Compared to the high elevation grid, low elevation grid receives less seasonal accumulation which is less frequent but intense rainfall. High elevation area has more rain events (varying 91 to 105) than low elevation (range; 66 to 75) using 6hour minimum inter-event time. In high elevation maximum event rain rate is 67mm/hour but low elevation is 122mm/hour. Our results also demonstrated clear difference between the two grid cells not only in terms of rainfall magnitude and property but also on the accuracy of satellite rainfall estimates which could be attributed to topography. 3B42RT, 3B42V7 and CMORPH overestimated total 3hour mean rainfall in low elevation (with bias 1.2, 1.1and 1.5 and ME 0.2, 0.1 and 0.5 respectively). All underestimated in high elevation by 0.9, 0.8 and 0.7, and ME -0.2, -0.2 and -0.5 for 3B42RT, 3B42V7 and CMORPH respectively. The categorical statistics indicated that CMORPH performed better in its probability of detection (POD), but it is influenced by non rainy clouds. All products highly affected by miss rainy events on high elevation area and by more false alarms at low elevation area. From our results 3B42V7 is best in the low elevation and 3B42RT performed better in the high elevation area.

***KEYWORDS**: Topography; Elevation; Rainfall variability; satellite rainfall estimate accuracy*

1. INTRODUCTION

1.1 Background and Justification

Accurate observation of precipitation is essential to hydrological and water resources management applications. There is an increasing realization that the selection of the type of input precipitation is more important than the choice of the hydrologic model in terms of producing robust hydrologic simulations (Wilk *et al*., 2006). Traditionally rain gauge measurements are taken as the source of precipitation data. Even though they are accurate, they represent only point locations. Rain gauges are sparse and also showed poor quality measurements in the Blue Nile region. This is due to the fact that rain gauges require high establishment and maintenance cost.

Satellite rain fall estimate are becoming potential sources of climatic information especially in developing countries like Ethiopia. Hydrological models have potential information about available water resources. But, it is extremely difficult to establish models and generate representative water resources availability information without adequate accurate rain fall information. Satellite rainfall estimates can be available over large and remote areas with hydrologically appropriate spatial and temporal resolution. But they are subjected to errors and need verifications. Understanding errors needs availability of high quality ground based truth measurements. In this study automatic rain gauge network at a reasonable distance were installed. Indeed, the spatial variability of rainfall has been seen in the context of accurate areal average rain fall information.

Wouter *et al.,* (2006), pointed out that in addition to the stochastic nature of rainfall, precipitation may be influenced by the irregular topography. The large variability in altitude may increase the variability by means of processes such as rain shading and strong winds. Therefore, events in the tropics (particularly in mountainous environments) have large spatial variability over short distances. However, quantitative information on this variability is missing in tropical mountainous regions due to the lack of adequate ground observations. An experiment has been conducted in the Blue Nile to deploy automatic rain gauges to quantify spatial and temporal variability in two contrasting elevation grids.

We conducted the study within a 0.25^{o} x 0.25^{o} grid areas, which match with high resolution of satellite rainfall products, such as PERSIANN-CCS (Precipitation Estimation from Remotely Sensed Information using Artifical Neural Networks – Cloud Classification System; Hong et al. 2004) and CMORPH (NOAA's Climate Prediction Center MORPHing technique; Joyce et al. 2004) and Tropical Rainfall Measuring Mission (TRMM) Multi-Satellite Precipitation Analysis (TMPA 3B42) version7 research product, near real time TMPA 3B42RT (Huffman, 2007).

In this work, TRMM Multi-Satellite Precipitation Analysis (TMPA 3B42) products: near real time TMPA 3B42RT and TMPA version7 research product and the CMORPH were evaluated. To evaluate the satellite estimates, 9-10 rain gauges were deployed within two contrasting elevation 0.25^{o} x 0.25^{o} grid areas. The number of events detected by single sensor only is significant indicator that the rain fall may not be uniform even for a single grid. This also supports the need to have closely knit net works of ground stations within the grid area.

According to Nesbitt *et al*. (2004), ground estimates tend to show modest increasing values of maximum precipitation with decreasing elevation. Tufa *et al.*, (2008), also evaluated two satellite rainfall estimation algorithms, CMORPH and TMPA over mountainous regions, in Ethiopia highlands. The study was conducted based on interpolating only one gauge to 0.25^{o} grid. The result indicated that the satellite rainfall estimates underestimated in the region.

Studies also showed that the accuracy of satellite rain fall estimation vary with region and also based on elevation. So, evaluating the accuracy of satellite rainfall estimates using very fine resolution ground based data will have importance for satellite rainfall estimation errors characterization.

1.2 Statement of the Problem

Satellite rainfall estimates are sources of climatic information; like precipitation data. These observation data can be incorporated with ground observations to use their spatial and temporal coverage. They can also be source of data especially in developing countries and remote areas.

Recent studies show clear signal on topography dependent error characteristics of high resolution satellite rainfall estimates in the complex terrain region of the Blue Nile. A significantly large overestimation by most widely used satellite estimates in lowland areas was reversed to underestimation in high elevation areas. This reversal of error was observed based on few ground based observations and at large temporal scale. The need for deployment of dense rain gauges to collect data at resolutions that matched with the high resolution satellite estimations was critical for this study. Understanding and quantifying spatial and temporal rainfall variability at the contrasting elevation locations can be important information in quantifying the errors associated to the satellite estimates.

1.3 Research Questions

In this study the following research questions have been addressed:

- What is the temporal and spatial rainfall variability at the two contrasting elevation location grids?
- What is the effect of topography on rainfall variability and accuracy of satellite rainfall estimates?
- How good are satellite rainfall estimations across contrasting elevation locations?

1.4 Objective of the Study

General objective

To quantify spatial and temporal rainfall variability and to evaluate the effect of topography on accuracy of satellite rainfall estimates using newly deployed dense rain gauge networks in Blue Nile basin.

Specific objectives

- To quantify the spatial and temporal rainfall variability within high resolution satellite pixel using ground based rainfall measurement from dense rain gauge networks.
- To investigate the effect of elevation on spatial rainfall variability.

- To compare high resolution satellite rainfall estimates against fine resolution ground truth measurements.
- To conduct inter-comparison among the satellite rainfall estimates.

1.5 Significance of the Study

Objective of the study was quantifying rainfall variability and evaluating accuracy of high resolution satellite rainfall estimates in contrasting elevation areas. The study sites are located in the lowlands and highlands of the upper Blue Nile basin. The study was emphasized on spatial variability of rainfall and influence of topography. The relative performance of satellite rainfall in the two locations has also been evaluated. Therefore, the result of this work over the aforementioned locations can enabling to adjust satellite rainfall estimates to provide accurate climate/ rainfall information for users of the data. The beneficiary of the study result believed to include; researchers, climate studies, farmers, water resources planners and managers and for disaster (like flash flooding) forecasting officers. Moreover, it is also thought to be transferred to other sites with the same topographical nature and climate condition in which the study is done.

2. LITERATURE REVIEW

This chapter of the paper contained background information related to the area of study. Outputs and drawn generalization ideas from different related research works are compiled here. It is shown in three sections separately as follows; spatial rainfall variability section, temporal rainfall variability and satellite rainfall estimate validation sections.

2.1 Temporal Rainfall Variability

The knowledge of variation of precipitation over short timescales, such as the diurnal cycle, is essential in understanding of the physics of the tropical atmosphere. In principle, the diurnal cycle of tropical convection can be interpreted as a response to heating of the surface earth due incoming solar radiation. As surface temperatures rise, the resulting convection increases reaching a maximum in the late afternoon or early evening. With surface cooling at night, convection decreases reaching a minimum in the early morning. At the night time cooling of existing cloudiness may result in destabilization and a secondary convection maximum during the night. There was a conclusion drawn from measure of temporal variability done in San Francisco (http://tornado.sfsu.edu/...) stated, rainfall with less CV is more dependable than that at higher CV. This smaller CV is reliable to use the average rainfall as an estimate for what might occur at any time scale than with higher CV. Rainfall with higher CV is characterized with more extremes (more dry and wet time alternating).

The differences in radiative cooling between convective regions and surrounding clear regions might intensify circulation and convection more during the night than during the day. (Wouter *et al*., 200) The diurnal cycle of precipitation in the tropical Andes of Colombia was characterized. Following general conclusions were drawn: (i) the observations indicate the existence of seasonally varying diurnal cycles. However, these cycles are highly variable in space; (ii) daily precipitation minima are found pre-dominantly during the late-morning hours of (0900–1100 LST) regardless of season and location; (iii) over northeastern and western Colombia, precipitation maxima occur predominantly in the afternoon; (iv) over the western

flank of the central Andes, precipitation maxima occur either around midnight, or during the afternoon, or both; and (v) over the eastern flank of the Central Cordillera, precipitation maxima occur around midnight. These indicate that highly variable topography plays a major role in determining the observed diurnal cycles, yet the identified seasonal variations of diurnal precipitation maxima cannot be explained by relief alone. The researchers identified strong time – space variability in the diurnal cycle of precipitation in the tropical Andes of Colombia results from a combination of local- and large-scale environmental conditions. These findings need to be merged with diagnostic studies of the diurnal cycle in tropical precipitation derived from satellite estimates, and also from general circulation (GCM) or meso-scale models. They can also be used to improve modeling and forecasting of tropical convection over land, but also serve as ground truth for satellite estimated rainfall and clarify the space – time dynamics of tropical precipitation over complex terrain.

2.2 Spatial Rainfall Variability

To minimize the error in recording precipitation at all times and locations appropriate gauge network design is important. There are three types gauge location determination within the catchment 1) random gauge location 2) systematic sampling for gauge location using specific distance between the gauges and 3) locating rain gauge by means of stratified random sampling using topographic characteristic (altitude, aspect, exposure and slope and rise) as basis to stratifying (James , 2001). High intensity rainfall events have more absolute spatial variability (e.g., standard deviation) and less relative spatial variability (as measured by coefficient of variation), compared to lower intensity events. (Menberu *et al.*, 2008; Reichardt *et al*., 1995) the coefficient of variation varies from 12% to 320%, with a median of 50%, indicating that there is a significantly large variability from one gauge observation to the other, and one gauge does not represent 5 km × 5 km grid-average daily values. A careful rain gauge layout design is critical to get accurate estimates at smaller number of rain gauges.

Due to the complex topography, organized weather systems are not common, and local convection, combined with orographical effects, plays a major role in the space–time

distribution of rainfall. Nesbitt *et al*., (2004) also generalized that, ground estimates tend to show modest increasing values of maximum precipitation with decreasing elevation.

2.3 Evaluation and Validation of Satellite Rainfall Products

2.3.1 Description of the satellite products

Some of the satellite precipitation products available and more commonly utilized products that cover large swaths of the planet include the National Aeronautics and Space Administration (NASA) Tropical Rainfall Measuring Mission (TRMM) Multi-satellite Precipitation Analysis (TMPA; Huffman *et al.*, 2007), and the U.S. National Oceanic and Atmospheric Administration (NOAA) Climate Prediction Center's (CPC) morphing technique (CMORPH; Joyce *et al*., 2004). The primary trend in the development of satellite precipitation products is to move toward merged datasets that take advantage of the best available data, regardless of source. There are three sources of satellite data. One; IR: this measures the brightness temperature. This is an indication of top cloud temperature and relate with cloud top height. Clouds with very cold temperature have deep convection. This convective associated with surface precipitation. The relationship between IR temperature and precipitation is indirect. Drawback of this source like others, it is impossible to discriminate non-rain cloud. Second; MW: precipitation can be inferred from active/passive microwave satellites. MW radiometers have several channels at 4 different frequencies for the Special Sensor Microwave/ Sensor (SSM/I), and 5 frequency for TRMM Microwave Imager (TMI) which ranges from 10-85GHz and which are polarized horizontally and vertically. Third one is; Multi-source data algorithm: involves combining different satellite observations. This improves average rainfall estimation. Examples are merged products of IR data from geo-synchronous satellites and MW data from low-orbit data. These merged sources benefit excellent time and space coverage from IR images and from direct connection of the MW observation with precipitation.

There are two TMPA 3B42, version 7 products in which monthly ground rain gauge data are applied to correct for bias adjustment and a real-time version (TMPA-RT) without gauge bias correction. The TMPA 3B42, version 7 product is merged based on the combination of

passive microwave (PMW) and infrared (IR) precipitation estimates from all available satellites with the utilization of PMW-calibrated IR-based rainfall estimates to fill PMW coverage gaps. The pure intermediate IR-based TRMM 3B42RT product provides a minimal latency (several hours) supporting near-real-time applications. CMORPH is similar to the TRMM products in that it merges satellite precipitation data from both IR and PMW sensors. But unlike TRMM-TMPA, CMORPH data are

i. Based on high resolution IR that is examined to estimate the motion of rainfall patterns to obtain a smooth morphing of PMW rain patterns between PMW snap-shots.
ii. CMORPH is a pure satellite product (no rain gauge correction). And
iii. Latency for the standard CMORPH product is 20–44 h (Kenneth *et al*., 2010).

The TRMM Multi-satellite Precipitation Analysis (TMPA) 3B42 version7 and real time (RT) product produces precipitation estimates by converting data from the TMI, SSM/I and the real time data from the Advanced Microwave Scanning Radiometer for the Earth Orbiting System (AMSR-E) using the Goddard Profiling Algorithm (Kummerow *et al.,* 1996). TRMM algorithm 3B42 provides adjusted 3 hour cumulative estimates of rain fall using merged microwave and Infrared precipitation information. All of the three satellite rainfall products have 0.25^{o} x 0.25^{o} spatial and 3 hour temporal resolution. Similarly, they capture longitudinal geographical coverage from 180^{o}W - 180^{o}E. But, their latitudinal geographical coverage differs; TRMM-3B42 V7 covers from 40^{o}N - 40^{o}S, TRMM-3B42RT has swath interval from 50^{o}N - 50^{o}S and 60^{o}N - 60^{o}S is for CMORPH.

2.3.2 Evaluation of TRMM3B42, TRMM 3B42RT and CMORPH and relevant works

The number of events detected by single sensor only is significant indicator that the rain fall may not be uniform even for a single grid. This supports the need to have closely knit net works of ground stations within grid area. Studies show that microwave algorithms such as used in CMORPH and PERSIANN overestimate precipitation in deep convective regimes (Nesbitt *et al.,* 2004). In the upper Blue Nile Gumero sub catchment only nine gauge stations had deployed in catchment area of 902sq.km. The purpose of the work was to validate

satellite estimate data and therefore to use as input in rainfall modeling (Ymeti, 2007). Evaluation of remotely sensed precipitation data products from TRMM3B42, TRMM 3B42RT and CMORPH can be carried out employing a range of statistical measures to quantify different aspects of the satellite precipitation product's performance (Mason, 2003). Statistical indicators and categorical statistics such as; bias of mean rainfall (Bias), mean error (ME), and mean absolute error (MAE) (indicators) and probability of detection (POD), false alarm ratio (FAR), critical success index (CSI), Hanssens and Kuiper discriminate (HK) use to assess each algorithm for its rainfall quantifying and occurrence detection skills. To assess objectively the skill of a sequence of rain- no rain estimates (e.g., whether or not a rain will occur or whether a rain rate will exceed a certain threshold), one first defines the 2 x 2 contingency table containing the total number of correct forecasts of occurrence (hits) A, the number of incorrect estimates of occurrence B, the number of incorrect forecasts of nonoccurrence C , and the number of correct forecasts of nonoccurrence D; (A, B, C, D) for (hits, false alarms, misses, correct negatives).

Dinku *et al*., (2008) seen the performance of CMORPH and TMPA over two mountainous regions, in Ethiopia highlands, Africa and Columbia highlands, South America. In the evaluation ground data was obtained by interpolating one gauge to 0.25^{o} x 0.25^{o} grid. The result was to be low in both regions. (Romilly and Mekonnen, 2011) stated that the microwave-based products TMPA 3B42RT and CMORPH outperform the infrared-based product PERSIANN: PERSIANN tends to underestimate rainfall by 43 %, while CMORPH tends to underestimate by 11 % and TMPA 3B42RT tends to over-estimate by 5 %. The bias in the satellite rainfall estimates depends on the rainfall regime, and, in some regimes, the elevation. In the northwest region, which is characterized mainly by highland topography, a humid climate and a strong Inter-tropical Convergence Zone (ITCZ) effect, elevation has a strong influence on the accuracy of the SREs: TMPA 3B42RT and CMORPH tend to overestimate at low elevations, whereas PERSIANN underestimates at high elevations.

Performance of TRMM 3B42 and CMORPH estimates were assessed by comparisons with ground data at a daily time scale (Cohen *et al*., 2011). The probability of rainfall being detected by the satellite appears with POD of about 0.6 and FAR of about 0.5. However, they cannot be expected to provide results identical to the gauge measurements. Because gauging stations provide point measurements observed over continuous periods of time, while

satellites deliver spatial averages based on intermittent rain rate estimates and they smooth localized phenomena. CMORPH being the less precise in terms of volume ratio than TRMM 3B42, and overestimating the rainfall by about 40%. The results presented in this paper underline the fact that rainfall input data have to be studied before modeling the hydrological behavior of a basin in order to know the size of rainfall events and their distribution through space and time. Moreover, they illustrate the very strong dependency of the satellite product quality with the region of interest.

3. MATERIALS AND METHODS

3.1 Description of the Study Area

This research has been conducted in Upper Blue Nile basin (Figure_1.a) in Ethiopia, east Africa. The study area covers two grids with contrasting elevation. Both grids covered equal area of 0.25^o x 0.25^o approximately 625 sq.km. Geographically they are part of large land mass that cover more than 199776.04sq.km, area of Abay basin (Tufa *et al*., 2008). The climatic condition is humid and it receives annual rainfall mostly from summer season which ranges from 1100 mm and 1200 mm. The major rain producing feature is the Inter Tropical Convergence Zone (ITCZ); however, topography complicates the rainfall patterns significantly. The annual rainfall pattern is very complex with some areas having rainfall for ten consecutive months; others receive rainfall just for a couple of months, while still others are characterized by two distinct rainfall seasons. About 19 stations were installed in the two sites of study. Data for the analysis was from 85 days rainfall observation during the monsoon summer from July 01 – Sept 30 (JAS), 2012. This is the wettest time of the year. These 19 automatic rain gauges are installed by systematic sampling method of network design with nine in the lowland and 10 in the highland areas. Grid location was chosen in such a way that they match with high resolution satellite rainfall products (such as, PERSINN-CCS, TRMM-TMPA 3B42 and CMORPHed) with 0.25^o x 0.25^o pixel size. The grid areas are apart by about 250km air horizontal distance. Individual cell has its own column (C) and row (R) number used as identification and calculated as follows:

Column number (C-longitude) = $East(West) exterem\ of\ interest)/0.25$ ---------- (1)

Row number (RR-latitude) = $(N - No\ rth\ edge\ of\ the\ place\ of\ \ interest)/0.25$ ----- (2)

= $(South\ edge\ of\ the\ place\ of\ interest)/0.25$ ---------- (3)

Where, *N* is the latitudinal geographical coverage of a satellite rainfall product above the equator. Its value is 50^o, 40^o, and 60^o for TRMM-3B42RT, TRMM-3B42V7 and CMORPH respectively. In this study the *N* value was used because Ethiopia as a whole is found above the equator (0^o). The column and row identification of a grid (pixel) differs depending on the geographical coverage of the satellite product (see Appendix II: Table 1).

3.1.1 Low elevation grid

It is located in the central part of Benshangul-Gumuze Regional State with geographical attributes of 35.25^{o} to 35.50^{o} longitude and 11.00^{o} to 11.25^{o} latitude which is about 800 km West of Addis Ababa. Specific site of the Grid is Guba woreda, Metekel zone. It covers part of the Gilgel Beles river basin. The grid overlaps satellite pixel which has identification (column, row) numbers as described in above equation. The elevation of the stations ranging between 614m and 734m asl. The site has an average elevation of 695 m asl (average elevation of all stations) which is part of the lowest elevation area in the Abay basin (Figure_1 b). Because of having lower elevation the area is too warmer and weather condition even during the rainy season is hotter. The area is covered with temporal green forest; the trees exist only during the rainy time. No studies have been done in this low elevation site using ground truth data.

3.1.2 High elevation grid

This is a second study site in the highlands of Upper Blue Nile basin found 200km south of Bahir-dar city (capital of Amhara Regional State) with geographical location ranging from 37.25^{o} to 37.50^{o} longitudinal and 10.75^{o} to 11.00^{o} latitudinal. It inter-connects four woredas (Sekela, Quarit, Dega damot and Jabi Tehnan from west to right) in west Gojam zone. Grid size matches with very fine spatial and temporal resolution satellite rainfall estimates. The average elevation of the area (from elevation of stations) is 2097m asl which is within the Birr catchment. The elevation difference within the sub-grid varying from 1924m to 2631m asl. This grid is part of the highland area in the Abay basin (Figure_1 b).

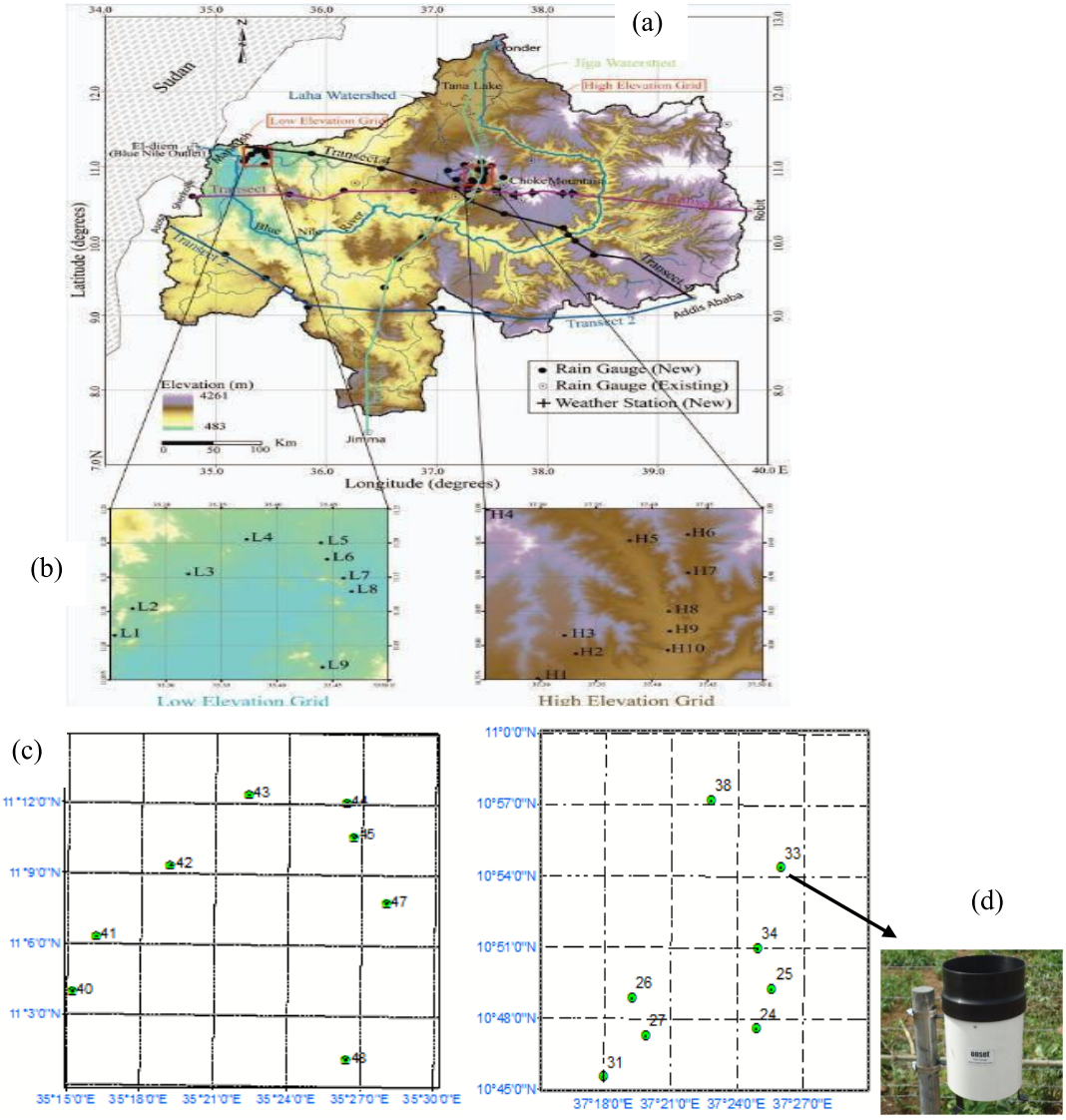

Figure 1: DEM of study regions. (a) DEM of the grids within upper Blue Nile and, (b) Location of the installed gauges (L=Low elevation and H= High elevation) (c) Location of the working rain gauges, (d) typical instrument setup.

3.1.3 Experiment campaign

This work is part of the team work in Upper Blue Nile basin in which about 53 new automatic tipping rain gauges and 5 new weather sensors are deployed. We have been performed a field work activity in June, 2012 stayed for about a month. This was to deploy the automatic rain gauges in the specified grid locations. First, preliminary assessment was conducted together with my advisor Dr. Menberu Meles Bitew to select appropriate location of the two grids (see Appendix I: Fig_1) within the basin. Nine and ten rain gauges were installed in low and high elevation grids respectively though designed number of rain gauges to be installed in each grid was 20. Both sites have area of about 625sq.km.

3.2 Materials Used

General description and use of the materials used in the research work is well explained as follows:

i. Nineteen automatic rain gauges were installed in two 0.25^{o} x 0.25^{o} grid sites, nine in the low elevation and ten in high elevation grid, in the Blue Nile (Fig_1 (b)). They are RG3 type rain gages, tipping bucket with a resolution of 0.254mm or 0.01inch per tip. They are mounted on a metal stand 1.5 m above soil surface and fenced using beam wire on a of 4m x 4m plot area. A sample of labeled gauge is shown in Fig_1 (d). Selection of station location was done in such a way that they are free of any external interference like: trees, vibration from roads and intervention due to agricultural activity. Distance between the gauge point and barrier is at least four times the height of the obstruction as shown in Appendix I: Fig_2. This work was difficult to follow a designed pattern since the areas were densely forested and undulating nature of topography. This character of the field forced us to install only 19 out of 40 (designed number) rain gauges for the two satellite pixels.

ii. Magnetic water level was utilized to check the verticality of the metal stand so that the funnel of the gauge should be on horizontal position.

iii. GPS has also been used to identify the geographical location and elevation of rain gauge station during time of installation. Second activity was collecting automatically recorded data from the rain gauges.

iv. Personal Computer (Laptop) and magnetic data logger (shuttle) with its USB cable were used to launch the automatic rain gauges and later to download the recorded data directly from rain gauges.

3.2.1 Specific description of the rain gauge

General information of the gauging stations such as station name, geographic locations (the longitude, latitude, and elevation), length and temporal scale of observation of the stations are provided in Table-1 below. The latitude and longitude of the stations are according to WGS84 coordinate system.

Table 1: General information of the gauging stations in the two grids (according to WGS84 coordinate system).

Code	Station Name	Longitude°	Latitude°	Elevation m asl	length of observation	Temporal scale
40	RD departure	35.2540	11.0649	722	85 days	15 minute
41	Alemayehu	35.2700	11.1040	734	85 days	15 minute
42	Abujar	35.3203	11.1547	677	85 days	15 minute
43	Yabulu	35.3727	11.2053	703	85 days	15 minute
44	Abraham	35.4396	11.2004	726	85 days	15 minute
45	Yetzig	35.4450	11.1762	712	85 days	15 minute
46	Babzenda	35.4599	11.1487	669	85 days	15 minute
47	Nasir	35.4672	11.1293	614	85 days	15 minute
48	Jalot	35.4410	11.0184	707	85 days	15 minute
		High elevation grid				
31	Dangber	37.2996	10.7470	2067	85 days	15 minute

Continued from Table 1

27	Amstegna	37.3317	10.7881	2094	85 days	15 minute
26	Maksegnin	37.3213	10.8147	2184	85 days	15 minute
24	Atiha	37.4144	10.7930	1924	85 days	15 minute
25	Genetabo	37.4162	10.8209	1936	85 days	15 minute
34	Senebo	37.4153	10.8498	1985	85 days	15 minute
33	Bahta	37.4326	10.9060	2047	85 days	15 minute
29	Ajale	37.2500	11.0000	2613	85 days	15 minute
38	Lebagedel	37.3800	10.9532	2013	85 days	15 minute

3. 3 Data and Method of Data Analysis

To achieve the stated objectives, data were collected from two rainfall observation sources for the two study areas: Data from dense automatic recording rain gauges with very fine (15 minutes) temporal resolution in .HOBO format. They are directly downloaded at the field with the help of personal computer and magnetic data logger. Second, data from three freely available remotely sensed high spatial and temporal resolution satellite rainfall estimates with 3hour temporal resolution and 0.25^{o} x 0.25^{o} spatial resolution.

3. 3.1 Rain gauge data observation

We deployed automatic rain gauges within Blue Nile basin and collect rainfall data over 2012 summer monsoon (wettest time) from July 1, 12 to Sep 30, 2012. Because of the launching date difference, we started analysis from July 8, at which all gauges uniformly started recording except one rain gauge failed with unknown reason in each site, and one has not full (45 days) observation time in low elevation area.

Nine rain gauges were used There were in low elevation and 10 rain gauges in high elevation grid area for the summer monsoon season, July 8 to Sep. 30, 2012. Data were converted to

excel format. For analysis purpose, data time series were aggregated to different (30min, 1hr, 3 hr, 6hr, 12hr, and daily) temporal scales for each station.

3.3.2 High resolution satellite rainfall estimates

Three remotely sensed satellite rainfall products; two TRMM - TMPA 3B42 products and the CMORPHed, were used. TRMM 3B42 is NASA's standard precipitation product, which is produced since 1998. It uses passive microwave (PM) emissions data sources from low oribital satellite observation data and infrared (IR) from geosynchronous in four steps: (1) PM estimates are calibrated and combined, (2) IR estimates are computed using PM estimates for calibration, (3) PM and IR estimates area combined and this become as final rainfall estimation, (4) data are rescaled to monthly total using Global Precipitation Climatology Centre (GPCC) data (Huffman et al., 2007). The estimates are released on a 0.25^{o} by 0.25^{o} grid at 3-hourly temporal resolution (00:00, 03:00,. . . , 21:00 UTC) in a global belt extending within 50^{o} N to 50^{o} S. The TRMM 3B42 is available in two forms of data. They are as TRMM-TMPA-3B42-near Real Time (RT) and TRMM-TMPA-3B42 Version 7 (V7) which is adjusted using ground data.

Their differences between these two data can be seen as follows: The near Real Time TRMM product 3B42 RT is being computed with the TMPA in near real time, and constitutes the timeliest source of TMPA estimates. The complete 3B42 RT data record is not reprocessed as upgrades are made to the procedure; its main focus is timeliness of data availability. In near real time it is not possible to apply precipitation gauge data to correct for bias adjustment. Note that 3B42 V7 estimates are considered to replace the 3B42 RT estimates as each month of the 3B42 data are computed during the following month. The 3B42 V7 processing is designed to maximize data quality, so 3B42 V7 is strongly recommended for any research work not specifically focused on real time applications.

CMORPH is constructed from similar inputs as those used in TRMM 3B42 with the difference that it does not merge PM and IR rain estimates. It involves calibration of IR estimates using PM estimates. Therefore, at times and locations when PM data are unavailable, it uses the motion vector derived from half-hourly geostationary satellite IR data

to interpolate precipitation (Joyce *et al*., 2004). Therefore, analysis does not rely on IR data for direct rainfall estimation. The original product of CMORPH, starting in December 2002, has a very high spatial resolution: 8 km grid and half-hourly time step. However, historical data are available only at a spatial resolution of 0.25^{o} and at 3hour temporal resolution (00:00, 03:00,… 21:00 UTC) in a global belt extending from 60^{o} N to 60^{o} S. General data set description of the products used in this study is summarized in Appendix II: Table 1.

Remotely sensed rainfall data were downloaded from freely available web portal of NASA through anonymous FTP in different formats. These are with 0.25^{o} spatial and 3hour temporal resolution. These products are available with 40^{o} N- 40^{o} S (TRMM-TMPA-3B42 V7), 50^{o} N - 50^{o} S (TRMM-TMPA-3B42RT) and 60^{o} N - 60^{o} S (CMORPH) latitudinal coverage. The longitudinal geographical coverage of all the three is from 180^{o} west to 180^{o} east.

Satellite rainfall estimate data have been collected for the same space and time which match with ground rainfall data, summer monsoon season July 8 to September 30, 2012. Interpretation of these data sources was processed using computer programming known as the Interactive Data Language, IDL.

To compare the rainfall estimates with ground truth, the high quality ground point measurement was interpolated to grid areal rainfall value. Rain gauge value which is the representative ground areal rainfall was calculated using thiessen polygon. McCuen (1998) stated that thiessen polygon method is essentially used for estimation of areal rainfall. There is an assumption that every single gauge represents a flat polygon. This method amounts at drawing around each gage a polygon of influence with the boundaries at a distance halfway between gage pairs. The reason to select this method than arithmetic mean value of the gauges is, there is significant elevation difference between the gauge stations in both areas of study. The representative spatial mean rainfall was obtained using the following equation:

$$\sum_{i=1}^{N} \frac{Ri*Ai}{At} \quad \text{----------} \quad (4)$$

Where, *Ri* is rainfall value at gauge *i* at any temporal resolution; *Ai* is portion of area within the grid which is covered by gauge *i* calculated using ArcGIS software; *At* total area of the grid and *N* represent number of gauge stations within a grid. Fig_2 shows the polygons

constructed with their area of influence in fraction out of the total area 625 sq.km in the two grid areas.

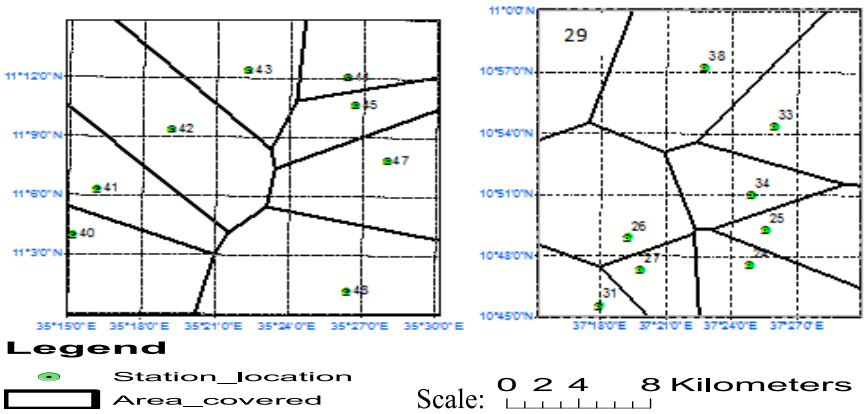

Figure 2: Thiessen polygons in low elevation (left panel) and high elevation (right panel)

The area coefficients represented by each rain gauge in both study areas are shown below.

Raingauges in low elevation area								
Station Code	40	41	42	43	44	45	47	48
Area covered	0.11	0.09	0.20	0.12	0.09	0.07	0.13	0.19

Raingauges in high elevation area									
Station Code	26	25	38	27	31	33	34	24	29
Area covered	0.17	0.08	0.20	0.05	0.06	0.16	0.08	0.10	0.10

3.3.3 Method of data analysis

We used statistical indicators and harmonic analysis for temporal and spatial rainfall variability and for satellite rainfall estimates evaluation.

The standard statistical indicators which have been used to analyze spatio-temporal rainfall variability include: total seasonal accumulated rainfall, spatial mean rainfall, temporal mean rainfall, conditional mean rainfall, percent of raining hour duration, spatio-temporal coefficient of variation, spatial correlation coefficient.

The total accumulated rainfall shows total rain depth that each rain gauge received during the study period (in the 85 days). Percent of raining hours (%) is the ratio of the raining hours (> 0 mm/hr) to the total (85days * 24hours = 2040) hours in the study period. Other indicators of spatio-temporal variability are temporal mean rainfall ($\overline{Ri}$), conditional mean rainfall. The two are temporal mean values. The difference is that, the former is simply calculated by dividing the total seasonal rainfall by the total number of hours in the study period, while conditional mean rainfall ($\overline{R}ic$) is the ratio of the total seasonal rainfall to the total number of raining hours (> 0 mm/hr). These two mean values show frequency and to some extent the intensity of rainfall at every gauge station. Example, gauge with higher total seasonal rainfall (or mean rainfall) and smaller conditional mean value, receives frequent hourly rainfall. Spatio-temporal rainfall of each gauge (i) was also seen using coefficient of variation (CVi). This CVi shows the temporal rainfall variability at 15minute, 30minute, 1hour, 3hour and daily temporal scales for each gauge station. In (*http://tornado.sfsu.edu/...)* stated that, rainfall with less CVi is more dependable than that at higher CVi. This smaller CVi is reliable to use the average rainfall as an estimate for what might occur at any time scale than with higher CVi. Rainfall with higher CVi is characterized with more extremes (more dry and wet time alternating). Result of this CVi can also be a reference to choose time scale of ground data with which other (like; satellite rainfall estimates) sources will be compared. Harmonic analysis was applied to assess diurnal cycle of hourly rainfall in the two grid areas. The graph indicates the pattern and magnitude of rainfall within a day and therefore one can investigate source of rainfall.

Spatial mean rainfall, spatial coefficient of variation and correlation coefficient within each grid area were analyzed. A large spatial coefficient of variation (CVt) for a rainfall event at indicates that the variability is large. Its value is larger for small spatial mean rainfall because the mean value is small. Therefore, large spatial coefficient of variation does not necessarily indicate high rainfall variability between the gauges. To ignore these very small rainfall values from the analysis, we considered spatial mean rainfalls which had contribution to the XX% (example: 25%, 50%, and 75% ...) of the total seasonal accumulated rainfall. In this paper, rainfall values which have a contribution to the 50% and 75% of the total seasonal accumulated rainfall in the two areas of study were separated.

The relationship rainfall value of a gauge with all the rest gauges within the grid was assessed using correlation coefficient (CC). This also another spatial rainfall variability indicator and suggests on the density of rain gauge network within every grid.

The following statistical procedures were used for spatial analysis:

$\overline{R}_t = \frac{1}{n}\sum_{i=1}^{n} Rit$ ---------- (5) $St = \sqrt{\frac{1}{n}\sum_{i=1}^{n}(Rit - \overline{R}t)^2}$ ------ (6)

$CV_t = St/\overline{R}t$ ---------- (7) $CC\ (Ri, Rj) = \frac{\sum(Ri - \overline{Ri})(Rj - \overline{R}j)}{\sqrt{(Ri - \overline{Ri})^2\ (Rj - \overline{R}j)^2}}$ ---- (8)

Where, $\overline{R}t$ = spatial mean rainfall at time *t*, n = number of rain gauges within the grid, R*i* = Rainfall value at gauge i, St = Spatial standard deviation, *t* is time scale and *i* is a gauge. Rj rainfall value and *j* stands for the gauges in the grid (j = 1, 2, 3, …, n-1).

Similarly for the spatio-temporal analysis was done using:

$\% = \frac{rain\ hours * 100}{Total\ observation\ hours}$ -------- (9) $\overline{Ri} = \frac{1}{m}\sum_{i=1}^{m} Rt$ ------ (10)

$\overline{R}ic = \frac{\frac{1}{m}\sum_{i=1}^{m} Rt}{r}$ --------- (11) $Si = \sqrt{\frac{1}{m}\sum_{i=1}^{m}\left(Rt - \overline{Ri}\right)^2}$ ----- (12)

$CVi = Si/\overline{Ri}$ ---------- (13)

Where, $\overline{Ri}$ = temporal mean rainfall of gauge *i*, $\overline{R}ic$ = conditional mean, S*i* = temporal standard deviation of gauge *i,* CV*i* is coefficient of variation for gauge *i*, Rt is rainfall value gauge *i* in time *t, m* is the number of observations and *r* is number of rainy hours during the study period. Raining hours are total hours in which the rainfall rained during the study period.

Event properties analysis based on 6 hour dry time with 15minute aggregated time were analyzed in the two grid areas. Event duration and rain rate may serve to identify events (cited in: Haile *et al*., 2011). In the same paper, it reviews a large number of criteria and reported that the applied minimum inter event time (MIT) varies from 3 min to 24 h while the minimum event depth varies from measurable amount (e.g. 0.254 mm for rain gauges used in this study) to 13.0 mm. To mark the start and end time of events in this study it was done

based on the minimum inter event time of 6hr that is if the length of a dry period between two gauge rainfall records exceeds 6hr then these records will be identified as part of separate events otherwise these records form a single event. In characterization of the event properties, we used simple statistics to compute the event rainfall depth, mean event rate, duration of event rainfall and peak event rate.

3.4 Validation of Satellite Rainfall Estimate Products

To make comparisons of satellite rainfall with ground data, first we established data pairs from the two data sources. This is to eliminate the differences in the resolution of satellite precipitation fields and reference data fields. Standard and categorical indicators have been used to evaluate the satellite rainfall products. Standard statistics measure accuracy of a rainfall amount estimated relative to observed rainfall volume. However, categorical statistics used to verify rainfall event detection ability of an estimate regardless to rainfall amount. This presents statistics comparison of three satellite rainfall estimates with ground observation data.

Mean error (ME), mean absolute error (MAE), Bias (mean volume ratio) are the standard statistics measures. The categorical verification measures include: probability of detection (POD), false alarm ratio (FAR), critical success index (CSI) and Hanssen and Kuiper discriminate skill (HK) (Tufa *etal.,* 2008 and Mason, 2003).

$$ME = \frac{1}{N}\sum_{i=1}^{N}(S - R) \quad \text{---------- (14)} \qquad MAE = \frac{1}{N}\sum_{i=1}^{N}|S - R| \quad \text{-------- (15)}$$

$$Bias = \frac{\sum S}{\sum R} \quad \text{---------- (16)}$$

Where, R = rain gauge value from thiessen polygon method in mm, S = satellite rainfall value in mm, and N = number of data pairs. ME and MAE are mean error and mean absolute error in millimeters [mm], while Bias (mean volume ratio) does not have unit.

These measures show accuracy of the rainfall estimates relative to ground reference areal mean rainfall. Mean error (ME) is the mean of the differences of all data pairs. The ME with value of zero show accurate rainfall amount estimation. Positive and negative values indicate

overestimation and underestimation respectively. Mean absolute error (MAE) is the mean of absolute values of the errors. It is more robust measure of estimate accuracy and is somewhat more resistant to the presence of large outlier errors. Bias is also the ratio of mean estimated rainfall amount to the mean observed with value ranging from infinity to zero. The value of one shows perfect skill, while values less than one and greater than one respectively indicate underestimation and overestimation of the ground rainfall observation.

Another way of verifying the rainfall estimates is depending on their ability of detecting a rainfall event in comparison to observed event. These events can be from rainy or non rainy clouds. Therefore, to assess accuracy of the products whether they are affected by non rainy clouds or missing observed events, categorical statistics analysis have been applied. These include: probability of detection (POD), false alarm ratio (FAR), critical success index (CSI), hansens and kuipers discriminate (HK). These are used to see the ability of detecting rainfall events but not the rainfall amount. They use (2 x 2) contingency table of estimates and observations for the whole period of experiment. They are calculated as follows.

$$POD = \frac{A}{A+C} \quad \text{---------- (17)} \qquad FAR = \frac{B}{A+B} \quad \text{-------- (18)}$$

$$CSI = \frac{A}{A+B+C} \quad \text{--------- (19)} \qquad [\%] = \quad \text{---------- (20)}$$

$$HK = \frac{A}{A+C} - \frac{B}{B+D} \quad \text{--------- (21)}$$

Where A, B, C, and D represent hits, false alarms, misses, correct negative based on a 0.254mm reference rainfall. Perfect estimate produces only hits and correct negatives, with no misses and false alarm. In definition, *hit*s are the number of event estimates that correspond to event observations; *false alarms* is the number of event estimates that do not correspond to observed events; *misses* is the number of no-event estimates corresponding to observed events; *correct negative* is the number of no-event estimates corresponding to no events observed.

The terms can be seen in a contingency table (Mason, 2003), which is a two-dimensional table that gives the discrete joint sample distribution of estimates and observations in terms of cell counts. For categorical estimates, having only two possible outcomes (number of rains and no-rains), the following (2 x 2) table can be produced. Number of events for each category is

represented by A, B, C, and D. Where, N is the total number of pairs of estimates and observed.

Table 2: Schematic contingency table for categorical estimates of a rain - no rain event

	Event observed		
Event estimated	rain	no rain	Total
rain	***A*** (hits)	***B*** (false alarms)	A + B (estimates)
no rain	**C** (misses)	***D*** (correct negative)	C + D (no estimates)
Total	A + C (observed)	**B + D** (no observed)	$A + B + C + D = N$

POD is categorical estimate score equal to the total number of correct event hits divided by the total number of events observed. Reversely, FAR is verification measure of an estimate performance equal to the number of false alarms divided by the total number of events estimate. The CSI is relatively frequently used, with good reason. Unlike the POD and the FAR, it takes into account both false alarms and missed events, and is therefore a more balanced score. The CSI is somewhat sensitive to the climatology of the event, tending to give poorer scores for rare events. HK score has a range of -1 to +1, with 0 representing no skill. Negative values would be associated with "worst" estimates, and could be converted to positive skill simply by replacing all the yes estimate with no and vice-versa. The HK is also the difference between the POD and FAR. This format leads to a useful interpretation of the score as distinguishing between rain and non rain cases, and allows one to examine whether estimating an event, particularly a rare event more often leads to an important increase in false alarms or not. A drawback of this score is that it tends to converge to the POD for rare events, because the value of "D (miss events)" becomes very large. Value range, perfect value and the description of the parameters is described in Table 2 below.

Table 3: Description and value of the rainfall estimate verification measures.

Statistic	range value	perfect score	No kill	Description (value indicates)
Bias	0 to ∞	1	0 & ∞	Over/under estimation of rainfall amount
POD	0 to 1	1	0	Fraction of observed events that were correctly estimated
FAR	0 to 1	0	1	Fraction of "rain" estimates in which the event did not observed
CSI	0 to 1	1	0	Fraction of observed and/or forecast events that were correctly forecast.
HK	-1 to 1	1	0	Ability of estimate to separate "rain" cases from "no rain"

4. RESULTS AND DISCUSSIONS

According to previous sections, this part of the paper contains analysis results with their discussion. This is classified in to: spatial and temporal rainfall variability, rain event property and satellite rainfall evaluation sections.

4.1 Temporal Rainfall Analysis

Temporal rainfall variability of each rain gauge station was analyzed based on total seasonal rainfall, percent of rainfall duration, and mean rainfall over the whole study period, conditional mean of rainfall, coefficient of variation and the hourly diurnal cycle. Accordingly, they are shown as dotted graph at the location plotted using ArcGIS.

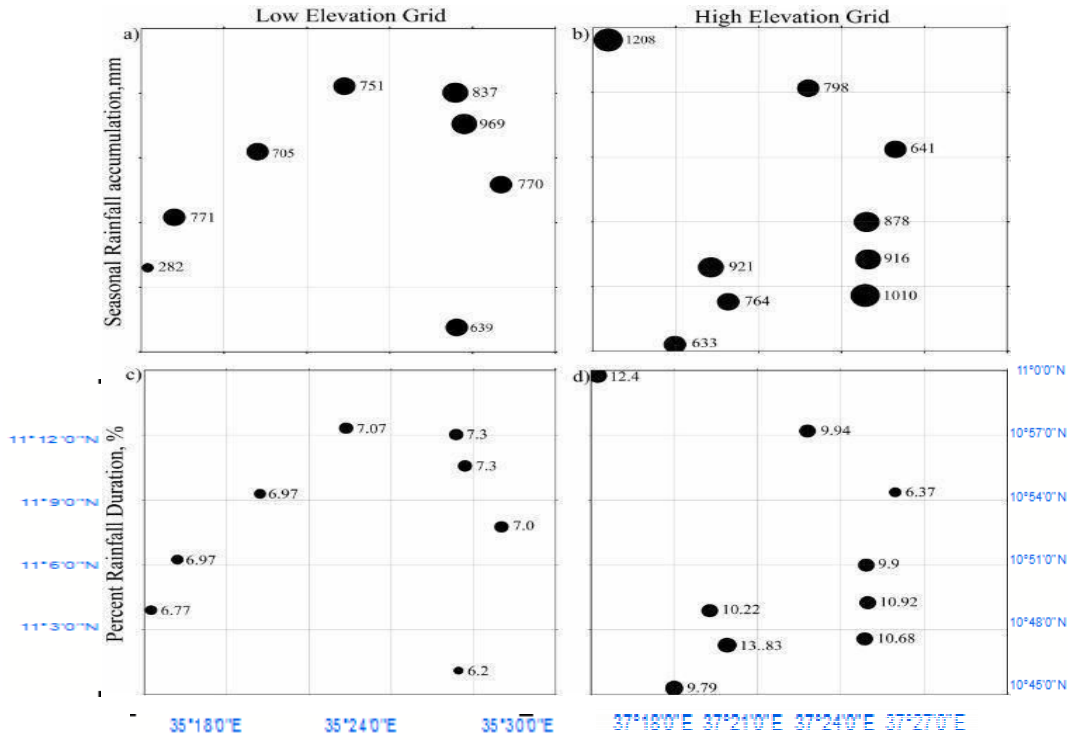

Figure 3: Seasonal accumulated rainfall (mm) and percent (%) of hourly rainfall duration. Left column (low elevation) and right column (high elevation)

As shown from (figure-3), high elevation grid obtained higher seasonal accumulated rainfall than the lower elevation during the same duration. The mean rainfall of low elevation varied from 629 mm (Gauge_48) to 969 mm (Gauge_45) value. But, in the high elevation area it varied from 633mm (Gauge_31) to 1208mm (Gauge_29). The total seasonal rainfall is highly variable in the mountainous area than the low elevation. The difference is height difference between the stations. Elevation of Gauge_31 is 2067m asl (near to mean value, 2097m) whereas Gauge_29 is 2631m asl which is the highest point of all stations. This indicates, there was high difference in volume contribution to seasonal accumulated rainfall from the area. In the percent of rainfall duration (fig_3 (d)), unlike the lower elevation high elevation had higher variability of percent of rain fall duration among rain gauges. In the mountainous area, its value varies from 6.4% to 13.8% whereas in low elevation area it ranges from 6.7% to 7.3% of the total analysis period. The difference was from the topography complexity of the area. Possible reason is, nature of the topography have influence in changing of climate variables such as rainfall within the area.

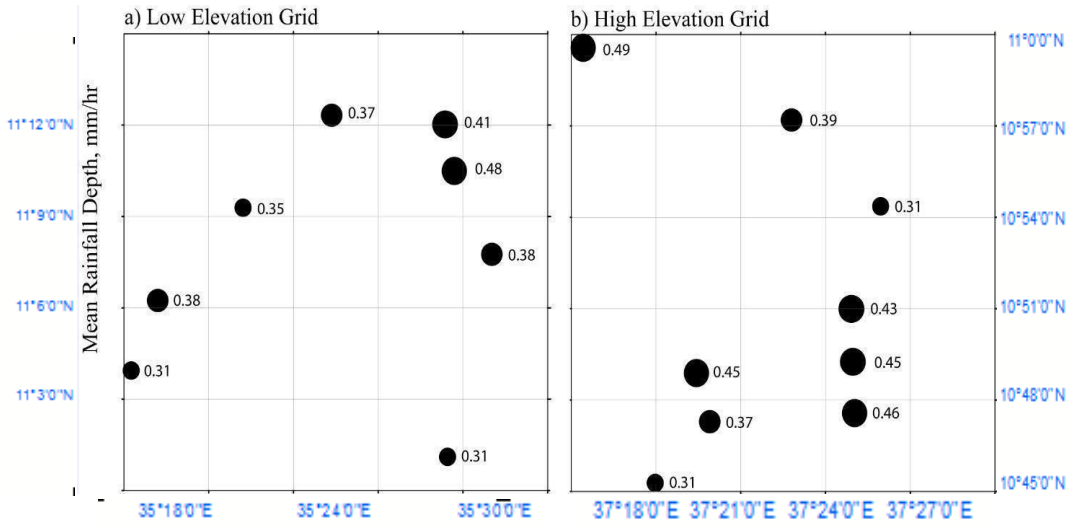

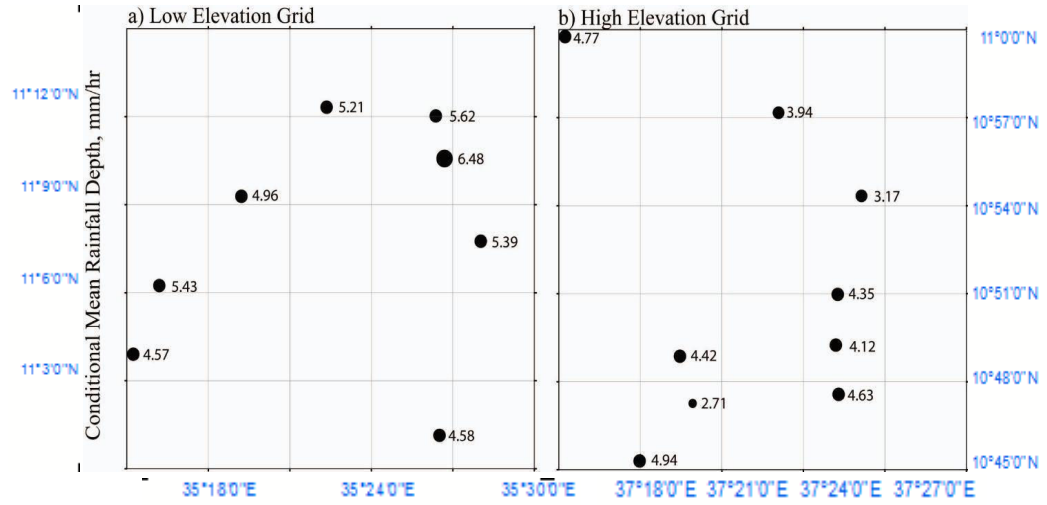

Figure 4: Mean rainfall depth and conditional mean rainfall depth in low elevation (left column), and high elevation area (right column).

The temporal mean rainfall depth indicated the ratio of total seasonal rainfall to total hours of observation during the study period. Whereas the conditional mean rainfall is total seasonal rainfall divided by the number of hours in which rainfall occurred. The mean rainfall depth in the lower area is smaller than the high elevation area for the same time records. Mean rainfall depth taught that there was high accumulated rainfall in the high elevation area. The conditional mean rainfall shows the hourly rainfall occurrence. Its value was greater in the lower elevation even for same mean rainfall depth in both sites (eg. Mean depth = 0.4; yields conditional mean of 0.56 and 0.40 for low and high elevation respectively). This indicated the highland area had frequent hourly rainfall. In the lowland area, station with greater mean (0.6mm per hour) rainfall depth had corresponding greater conditional mean rainfall (6.5mm per hour), but this did not worked for other site. Therefore, there was less number of rainfall occurrence but with peak rates in lower elevated area. Individual rainfall observation had significant contribution for the temporal accumulation than the high elevation.

Spatio-temporal rainfall variability analysis result form 85 days of observation at different time intervals is shown in Figur_5 in both low and high elevation areas. In both areas there is no clear relationship between elevation and temporal coefficient of variation.

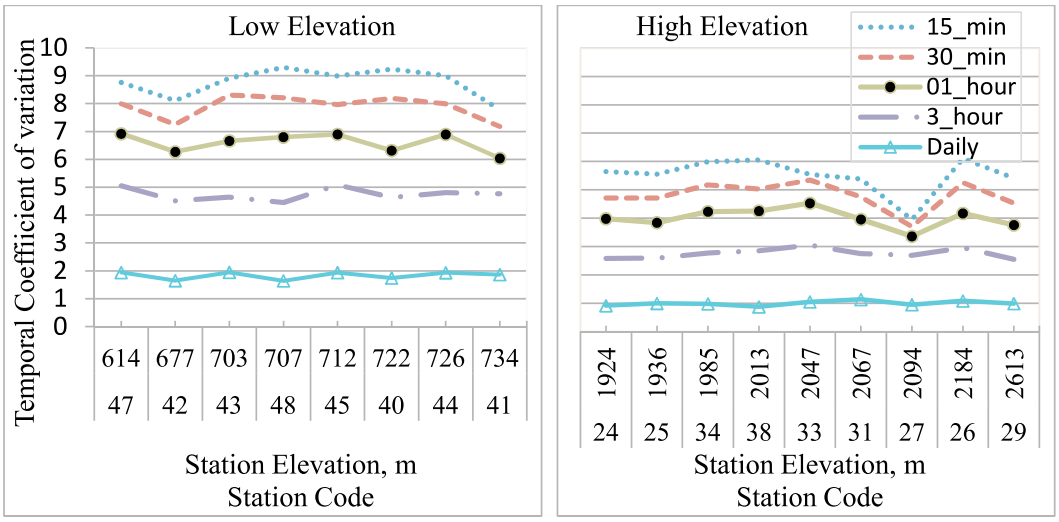

Figure 5: Spatio-temporal coefficient of variation at different temporal scales for each station.

Time interval of analysis is inversely related with coefficient of variation (CV). This is common characteristics of all rain gauges. (Fig-5), for similar temporal scale increment, CV value reduces rapidly in the lower elevation area. The seasonal accumulated rainfall is higher in the high elevation but less CV. This shows that, there was frequent (from the % of hours rainfall duration) with less extreme (less non rainy and less intensive) rainfalls in the highland. In contrasting the lower elevation, had more extreme and less frequent rainfall values. Therefore, from the above points, the dependable rainfall values in the two contrasting elevation study areas occur at different temporal scale. Dependable rainfall is a rainfall value with lesser CV one can be able estimate representative rainfall. In both sites the most dependable rainfall is at daily scale although they differ in precision. For example, to estimate rainfall in both areas with relatively same temporal precision (CV ~ 4.5), one can consider 3 hourly and 30 minute temporal resolution rainfall for low and high elevation area respectively. Another approach to the advantage of this result is in evaluation of satellite rainfall estimation products. It can be concluded that, for the comparison of satellite products, the time scale of the ground truth observation should be greater in the lower elevation grid to get better reference rainfall.

Average seasonal accumulated rainfall of low elevation and high elevation is 763mm and 905mm respectively. The graph of the diurnal cycle is plotted from the standardized difference using the mean value of the rainfall of 24 hours of the day. Low elevation area had two peaks hour values which contributed more to the total seasonal rainfall.

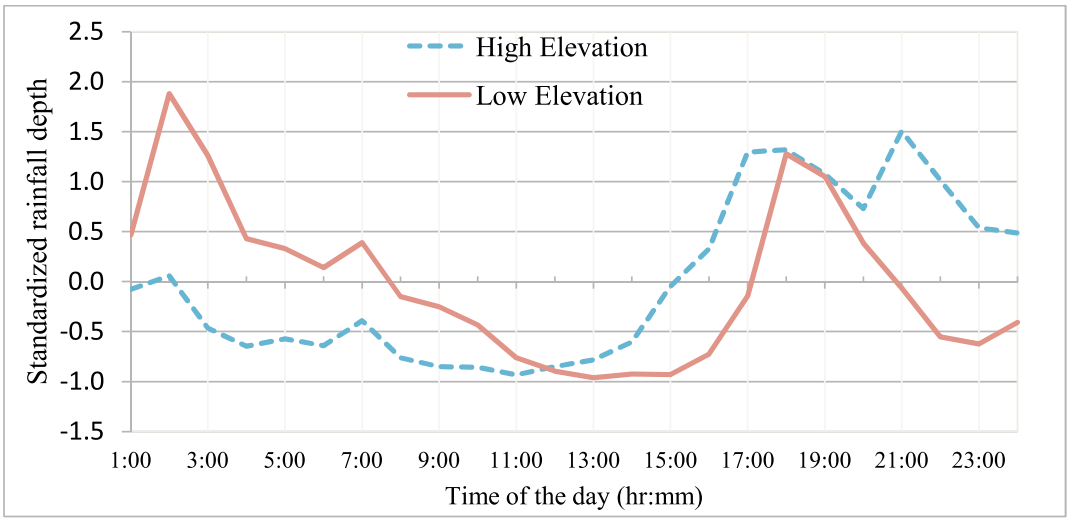

Figure 6: Diurnal cycle; low elevation- bold line and high elevation –dashed line during the study period.

Most of the rainfall rains at the late night (@0200 LST) with a peak standardized value of 1.9. There was also local maximum at late afternoon and early evening at 1800 with 1.3 and reduced quickly -0.55 at 2200 LST. During the morning time rainfall reduced slowly until 1300 to its absolute minimum (-1.0) value which remained for about 2hours. 60% of the total daily occurs from midnight (0000 LST) to the noon (1200 LST). Whereas, during late afternoon-late evening contributed only 40%.

The high elevation grid, though the rainfall follows similar pattern with low elevation, the amount of rainfall is quite different. In this site there is local maximum hourly rainfall at the midnight which gradually declined to prominent minimum (-.0.93) which corresponding 0.3mm/hr rainfall at late morning (1000). This minimum hourly rainfall was for an hour and tend to increase to another local maximum value of 1.3 at the evening (1700 through 1800 LST) and then to its absolute maximum value, 1.5, at late evening (2100 LST). These two

peak values are found in consequent times of the day. Most of the rainfall amount was contributed from 1500 (afternoon) to 0000 (midnight) LST with the 80% of the total seasonal rainfall and the rest (20%) is received from mid nigh until late morning.

When we contrast both areas, number of hour with equal or greater than their hourly mean rainfall is 10 and 9 for low and high elevation respectively. In the low elevation, gradual decrease of rainfall occurred from the sharp maximum during late mid night and reached minimum (zero) at the noon. This prominent minimum remained for three hours and rapidly increased to its local sharp maximum at the evening. Unlike the low elevation, high elevation area the local maximum at mid night decreased to absolute minimum (-0.93) at the late morning. But directly tend to increase. The high elevation received maximum peaks rainfall stayed for about 4hours from 1700 to 2100 LST.

From the standardized difference from the mean rainfall, it is evidenced that rainfall occurs during the whole day in high elevation area. However, rainfall in the low elevation grid area is influenced by extreme events. From this, nature of rainfall (rainfall frequency and intensity) is different in the two areas. Possible reasons might be, the high elevation area has temperature remarkably higher at day time than evening. This temperature at the afternoon can be an input energy in the lower atmosphere and induced convectional or orographic uplifts, and bringing an increase in cloud cover with rain and fog. Whereas, in low elevation area, in addition to the effect of temperature at the afternoon, the rainfall at the late night-early morning might be resulted from cloud movement (cloud circulation) from the Ethiopian highland due to pressure differences between the two air masses of the two areas.

4.2 Spatial Rainfall Variability Analysis

4.2.1 Spatial daily mean rainfall and spatial CV

Here daily time scale is used to assess the spatial rainfall variability; in terms of daily mean rainfall and spatial coefficient of variation (CVt). Fig_7 shows daily mean rainfall calculated using the thiessen polygon method and spatial CVt patterns in the two areas. From Fig_7 (a), it can be observed that there was huge variability of the daily maximum and minimum rain rate within the sub-grid. In low elevation area (with average elevation of 695m asl) the

extreme events were the most contributors for the total rainfall (which is 663 mm during the season). Maximum value of daily CVt indicates there were extreme values (more driest and wettest days). During the study period daily rain fall varied from 0mm to 62mm with 8mm mean daily rainfall. There were four non-rain days in the low elevation area. From the mathematical computations, the CVt of days having small spatial mean daily rainfall is exaggerated. This does not necessary explains that there was high rainfall variability in the grid. Because, in small rainfall events slight difference in spatial variability shows in large coefficient of variation because of small spatial mean value. Therefore, we limited the spatial analysis to raining days which had contribution to the 75% of the total seasonal rainfall.

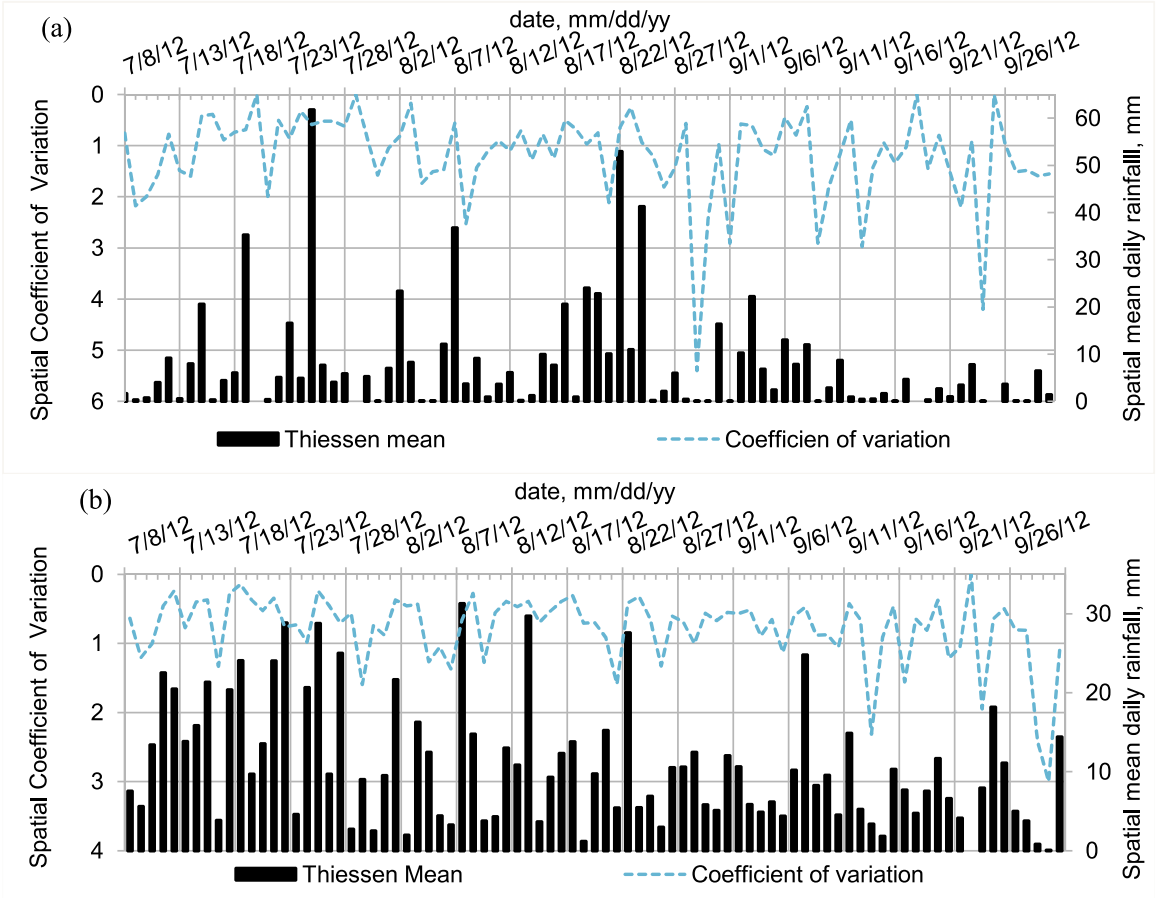

Figure 7: Spatial mean daily rainfall (bold line) and coefficient of variation (dashed line). (a) low elevation, and (b) high elevation area.

Whereas in the highland site (Fig_7 (b)) which has an average elevation 2097m asl, there are no distinguished extremes rather than frequent daily rainfalls. The total rainfall is 922mm with 11mm daily mean rainfall with mean daily rainfall varied from zero (only a day) to 31 mm/day.

Fig_8 showed that, there was a difference in contribution of each rainfall event to the total seasonal rainfall in the two areas. These enabling to assess the rainfall variability on other than zero rain days. For example, (Fig_8 (a & c)) showed 50% and 75% of the total seasonal rainfall in low elevation was contributed from daily rainfalls with or greater than 20mm/day and 8mm/day respectively. Indeed, percentage of daily observation number for 50% and 75% of the total mean rainfall were 11% and 25% respectively in the low elevation area.

Similarly (Fig_8.b and d), show 50% and 75% of the total spatial mean rainfall in the high elevation site over the study period was contributed from daily rainfalls with or greater than 14.5mm/day and 9.5mm/day respectively. Additionally, in high elevation grid it was discriminated that, 50% and 75% of the total seasonal rainfall was obtained from 25% and 47% of the total daily observations. This indicates, in lower elevation area the total spatial mean rainfall was contributed from heavier and less observations whereas in the high elevated area it was from large number of observation with frequent and light rainfall events.

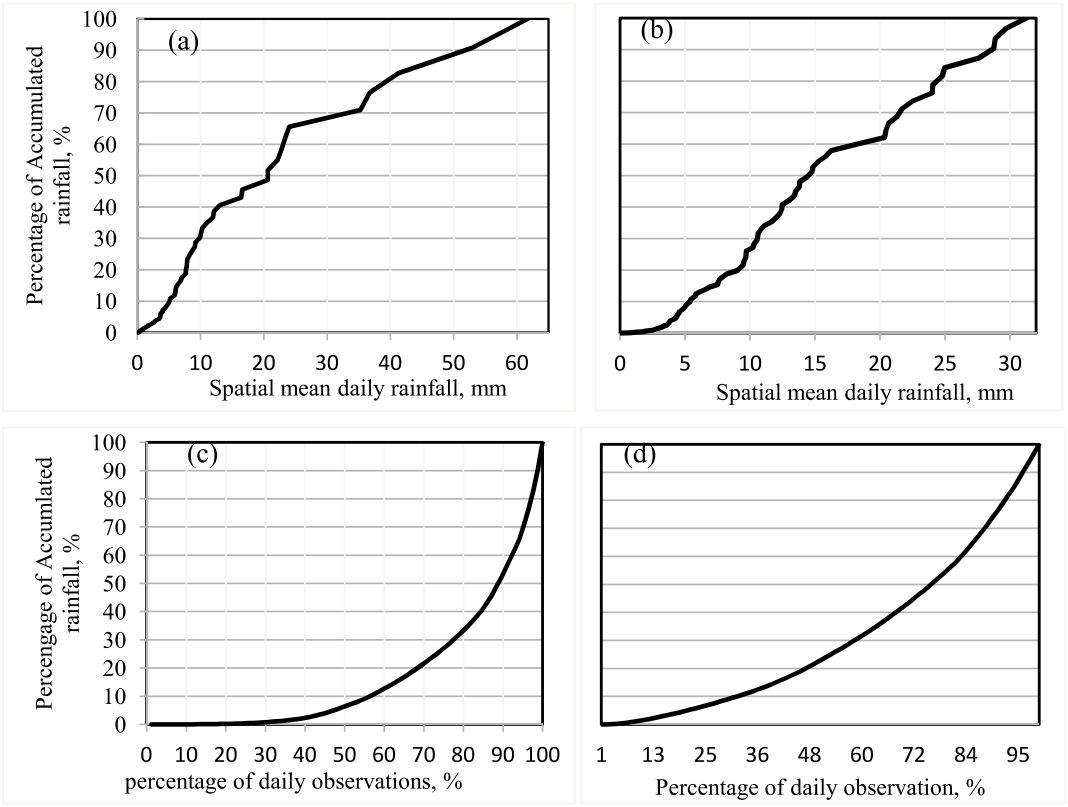

Figure 8: Percentage of accumulated seasonal rainfall (i): versus daily mean rainfall (a, b). (ii): versus daily number of observations; (a, c) for low elevation; (b, d) for high elevation grid.

From the above, in the same season (and time of observation) there was significant difference in rainfall properties in the two contrasting elevation grids. Each daily observation has substantial contribution in high elevation grid but this did not worked for the low elevation. In the later only some observations (days having peak wettest value) have greatest influence to total seasonal rainfall. In the study period, there was proportionality between the accumulated rainfall and number of observations in highland area. In other words, there was frequent and but less intensive daily rainfall in the region. The possible reason behind might be the convection process within the area due to the nature of the terrain elevation.

4.2.2 Spatial variability of daily rainfall using coefficient of variation

As explained in (Menberu, *et al.*, 2009), for small rainfall events slight difference in spatial variability results in large CVt because of small spatial mean value. It concluded that the CV of such small events is not practically interesting because the actual difference is negligible. Therefore, the analysis should be limited to the heavier rainfall value. We bounded the analysis to observations which have contribution to the 75% of the total seasonal rainfall in the grid sites. This result of statistical analysis is for all 85 daily observations. There is very large coefficient of variation for very small daily spatial mean rainfalls. Fig_7a (low elevation), the coefficient of variation varied from 17% in 3rd of August (with mean of 8.2mm/day) to 210% (with mean daily rainfall = 10mm). The median value CVt of 77% (corresponding for mean daily rainfall value 9.2mm was in the 7th of July.

On the other hand, Fig_7b, (high elevation) the magnitude of the daily CVt range from 15% on 18th of July having daily mean rainfall of 24mm to 127% on 4th of August (with mean daily = 12mm) with median value of 7% corresponding to rainfall value on 15th Sep with 10.3mm mean daily value. Let's see sub-grid and cross grid spatial rainfall variability based on three selected days from the two contrasting elevation grids (Table_4) for each gauge.

Table_4, (a; low elevation) shows daily observation with minimum CVt (17%), the individual deviation from the spatial mean daily rainfall (~8.2mm) varied from -15% (gauge 44) to 51 %(gauge 42). In July 12th, with daily spatial mean of 9.2mm and CVt of 77%, gauge stations varied from -97% gauge 48 to 150% gauge 42. In August 21st event (with CVt = 210%) the deviation from the mean (mean=10mm) from -90% (gauge 48) to 510% gauge 45.

Table 4: Spatial daily coefficient of variation on three selected daily observations between rain gauge stations in the two grids.

a.	**Station Code_Name (Low elevation grid)**								
Date	40_ Rdam	41_ Alemayehu	42_ abujar	43_ Yabulu	44_ Abraham	45_ Yetzig	47_ Nasir	48_ Jalot	Mean
i.	For the minimum daily CVt value ~ 17%								
8/3/12	-	10.2	12	9	7	8	9	8	8.2
Ri-$\bar{R}$d	-	2	4.2	1	-1.2	-0.2	0.8	-0.2	
%	-	24	51	12	-15	-2	10	2	
ii.	For the median daily CVt value ~ 77%								
7/12/12	-	23	15	14	7	9	10	0.3	9.2
Ri-$\bar{R}$d	-	14	5.8	4.8	-2.2	-0.2	0.8	-8.9	
%	-	150	63	52	-24	-2	9	-97	
iii.	For the largest daily CVt value ~ 210%								
8/21/12	1	9	16	2	12	61	3	1	10
Ri-$\bar{R}$t	-9	-1	6	-8	2	51	-7	-9	
%	-90	-10	60	-80	20	510	-70	-90	

b.	**Station Code_Name (High elevation grid)**									
Date	24_ Atiha	25_Genet abo	26_ Maksegnit	27_ Amistegna	29_ Ajale	31_ Dangber	33_ Bahta	34_ senebo	38_Leba gedel	Mean
i.	For the minimum daily CVt value ~ 15%									
7/18/12	31	27	25	22	20.2	19.8	25	25	22	24
Ri-$\bar{R}$d	7	3	01	-2	-4	-4	1	1	-2	
%	29	11	4	-9	-16	-18	3	3	-9	
ii.	For the median daily CVt value ~ 47%									
9/15/12	9.5	7.3	9.8	6.3	2.9	6.6	18	11	11.7	10
Ri-$\bar{R}$d	-0.5	-2.7	-0.2	-3.7	-7.1	-3.4	8	1	1.7	
%	-5	-27	-2	-37	-71	-34	80	100	170	
iii.	For the largest daily CVt value ~ 127%									
8/4/12	5.4	12.4	3	3	18.5	1.5	45.4	9.3	1.7	12
Ri-$\bar{R}$d	-6.6	0.4	-9	-9	6.5	-10.5	33.4	-2.7	-10.3	
%	-55	3.3	-75	-75	54	-87	278	-22	-85	

And section (b; high elevation) daily observation with less CVt (15%) the individual deviation from the spatial mean daily rainfall (~24mm) varied from -18% (gauge 31) to 29% (gauge 24). In Sep. 15th, with daily spatial mean of 10mm and CVt of 47%, gauge stations varied from -71% gauge 29 to 170% gauge38. In August 4th event (with CVt=127%) the deviation from the mean (mean=12mm) from -87% (gauge 31) to 278% gauge 33.

In low elevation spatial variability has random property and has no relation with elevation difference among gauge stations. But in high elevation grid, spatial CVt does have relation with elevation difference. For example, Ajale (elev. = 2613m) station over estimated the daily spatial reference rainfall and Lebagedel (elev. = 2013m) underestimated the spatial mean value.

4.2.3 Coefficient of correlation and distance

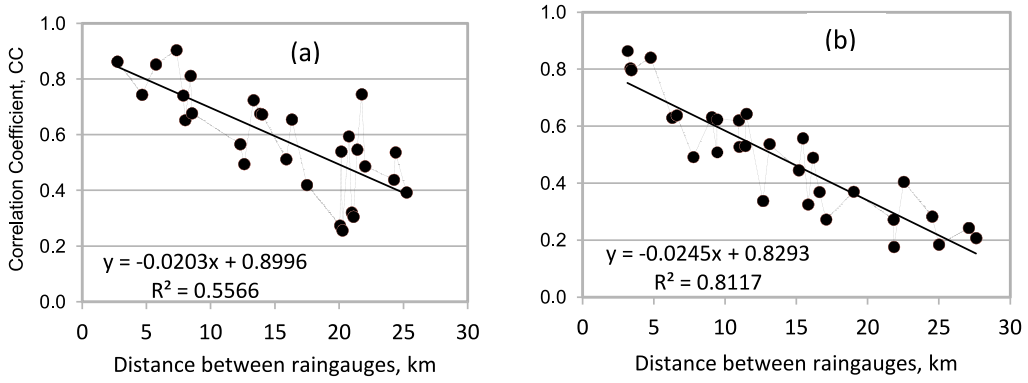

Figure 9: Bivarial analysis of the rain gauge stations; Correlation Coefficient versus mutual distance. (a) low elevation and (b) for high elevation grid.

(Fig-9.a) represents relationship between the mutual distance and coefficient of correlation of their daily rainfall value in the low elevation area. Rain gauges at a mutual distance less than 8km are strongly correlated, with coefficient or correlation (CC) higher than 0.74. However, even within this range, spatial variability in average rainfall is very high. Generally, even though there was gradual decrease of CC with increase of distance, there is no a specific relationship. In the low elevation area, rain gauges can estimate for 8km radius perimeter with

and greater CC of 0.75. Similarly, Fig-9 (b) shows rain gauges in the high elevation separated by less than 5km have very strong correlation with (or greater than) CC of 0.80. The relationship remains below 0.70 for mutual distances greater than 5km. Unlike low elevation (not specific trend), CC showed decaying with increasing horizontal distance. In the high elevation grid a rain gauge station can represent a radius of 5km with 0.8 correlations. Therefore, from the above we learn that (i) nature of rainfall is highly variable in the high elevation grid than the low elevation area due to the effect of complex topography and rainfall process. (ii) number of rain gauge network required should be dense in the high elevation area.

4.3 Event Properties Analysis

Fig_9 shows rain event properties of seven stations (85 days full recorded data) in the low elevation area. The area is located in the lowest elevation of the Abay basin with average elevation of 695m asl. Therefore, rain event properties at these gauging stations by terrain characteristics (Haile *et al.* 2011) with minimum inter event time of 6hour, the number of events varied from 66 to 75. In this sub-grid, a maximum 122mm rain event depth was occurred at gague-45 and minimum of 0.254mm in all stations with median value of about 4.4mm. The event is extreme event in the area. In terms of event duration, an event was stayed for maximum hour of 18, with minimum and median duration value of about 0.25h and 3h respectively. The maximum 15 minute peak rain rate in the area is 109 mm per hour. It has median value of about 5mm/h. In terms of event rain rates, it ranges between 0.1 mm/h and 30 mm/h with a median of about 1.5 mm/h. This show that, the middle value of the peak rain rate is about 4 times the median of mean event rain rate. The difference is, in MIT event time aggregated time scale there are more with no/less rain to the mean event rain depth.

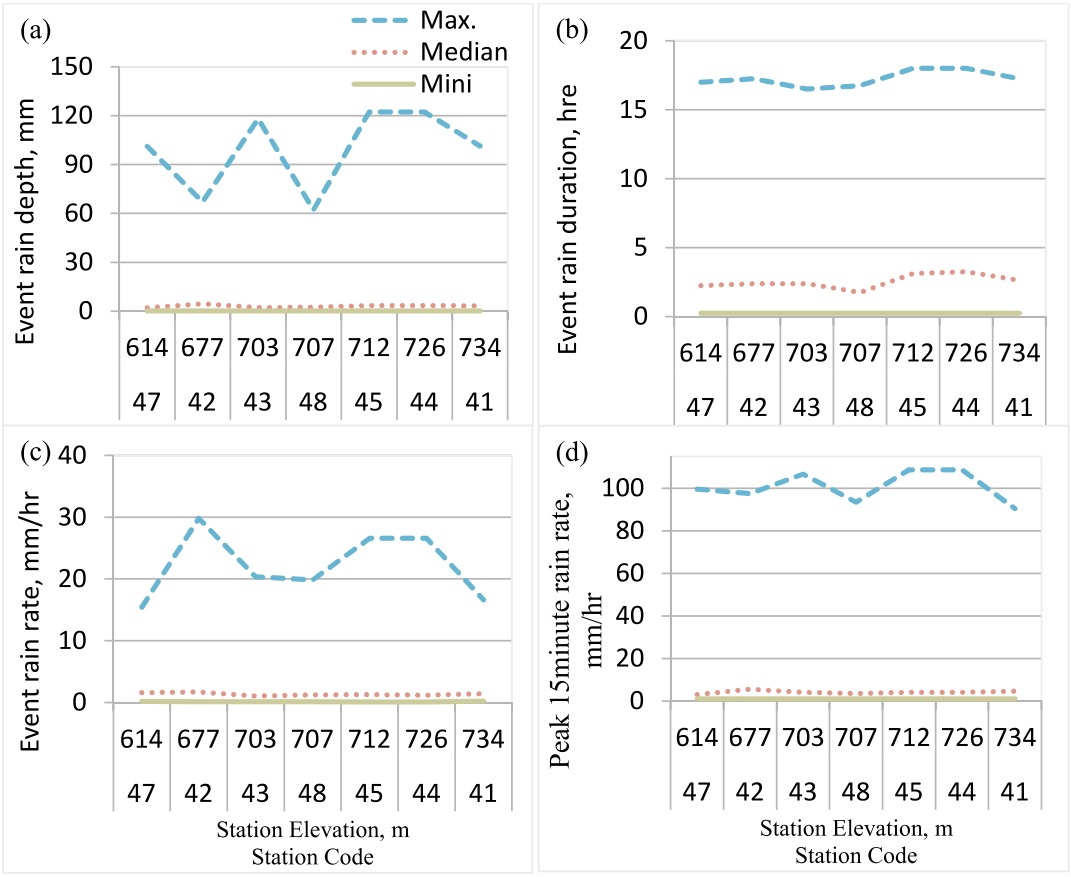

Figure 10: Rain event properties of seven stations in low elevation area. (a) total rain in all events in mm (b) event rain duration, hr, (c) rain event rate, mm/hr, and (d) peak event rain event, mm/hr.

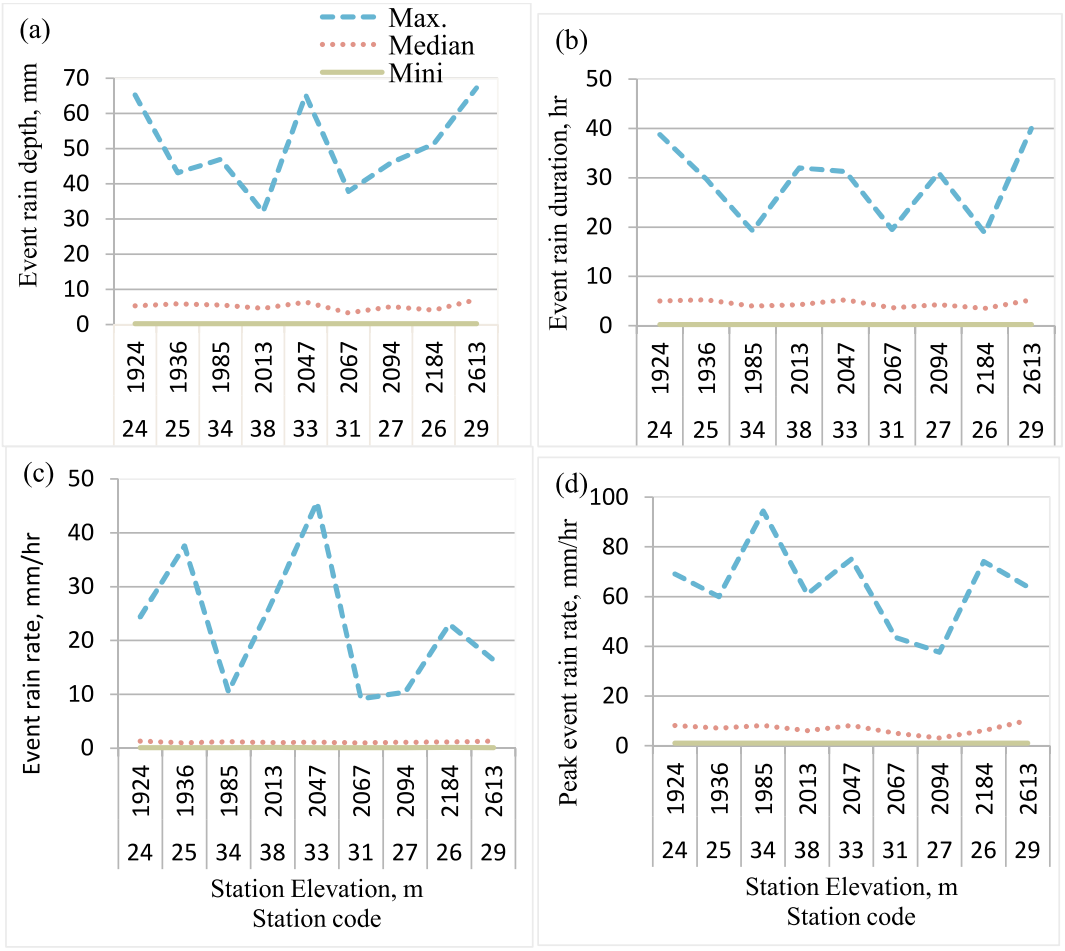

Figure 11: Rain event properties of nine stations in high elevation. (a) total rain in all events (mm), (b) event rain duration(hr), (c) event rain rate (mm/hr) and (d) peak event rain event (mm/hr).

Rain event characteristics for nine stations in the high elevation area (Fig_11) are shown. The area is part of highland area of upper Blue Nile basin with an average elevation of 2097m asl. Therefore, this is analyzing rain event properties at these gauging stations within the grid area. Based on time, t = 15 min aggregation scale and a minimum inter event time of 6hour, the number of events varied from 91 to 105. In this sub-grid, a maximum 67mm rain depth was occurred at gague-29 and minimum of 0.254mm in all stations with median value of about 5mm. The event is extreme event because which corresponds to the highest (with elevation of 2613mm) point in the area. An event was stayed for maximum hour of 40h, with minimum

and median duration value of about 0.25h and 4.5h respectively. The maximum 15 minute peak rain rate in the area was 95 mm/h. It has median value of about 7mm/h. Event rain rates range between 0.1 mm/h and 46 mm/h with a median of about 1.25 mm/h. This show that, the middle value of the peak rain rate is about 6 times the median of mean event rain rate. The difference is, in MIT event time aggregated time scale there are more with no/less rain to the mean event rain depth.

If we see the relation between elevation and event properties, in next section it has been seen that the rain event properties show relationship with terrain elevation considering both sites. As the elevation difference is insignificant between stations in each grid, this made to see both grids on a plot (where; scatter plots in the most left column are for the low elevation and the right one are for high elevation). A linear regression analysis was carried out to assess the relationship between elevation and rain event characteristics. The regression equations that are based on data from 16 (7 in low elevation and 9 in high elevation) stations are shown in Fig_12. The equations show that terrain elevation is positively correlated with rain duration, rain event depth and peak event rain rate, this is especially visible from station code 29 (Ajale: with elevation of 2613m) at high elevation grid. But, mean rain rate inversely related to elevation. Results indicate that events of short duration are not directly affected by elevation but when event duration increases, such may be due to effects of elevation.

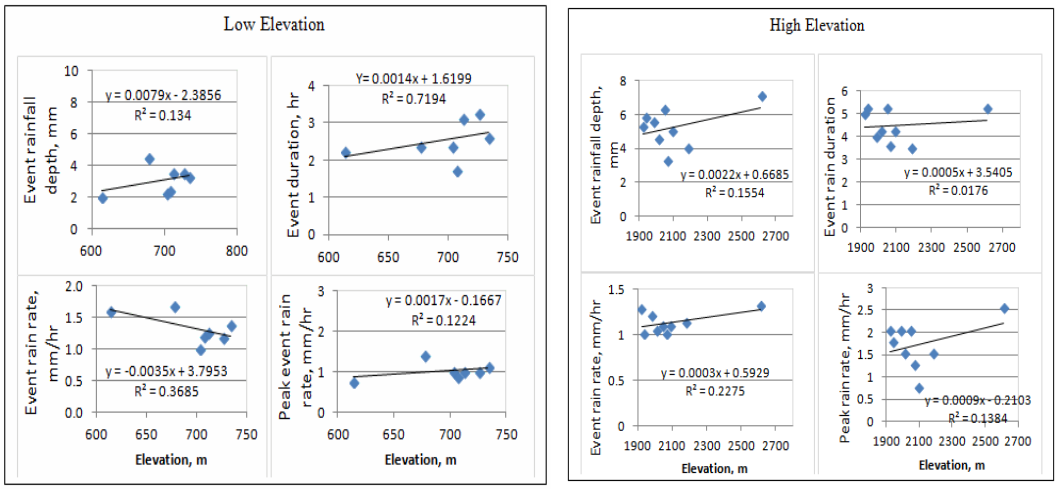

Figure 12: Relationship between rain event properties and elevation. (a) event rain depth, (b) event duration, (c) event intensity and (d) peak event rain rate.

4.4 Satellite Rainfall Estimates Evaluation and Validation

The validation result for three satellite products at 0.25° spatial resolution with different temporal resolution was analyzed. (Fig_13 and Fig_ 14) show the estimate errors as a function of time and observed rain rates to assess the error characteristics in both sites.

4.4.1 Different temporal scales at 0.25° spatial resolution in the two areas

The results show that the three products have poor performance in terms of pixel-by-pixel comparisons. Percentage of underestimation maximum rainfall decreases as the temporal scale become larger in both elevation areas. But, degree of underestimation is very high in high elevation area. For example, the estimates underestimated maximum daily rainfall in low and high elevation by about 67% and 98% respectively. Mean error (ME) values directly (increasingly) related with the time scale that is as temporal scale became coarser the ME increases. ME value in low elevation area is positive for all products indicating overestimating the actual rainfall. The three products were overestimated the rain fall. CMORPH highly overestimated followed by 3B42 RT. The mean bias also follows decreasing order for CMORPH, 3B42 RT and 3B42 V7 (with bias value of 1.5, 1.2 and 1.1 respectively; Appendix II: Table 2). 3B42 V7 works best in the low elevation grid area with a least mean error.

Therefore, one can conclude that the height of the cloud affects the accuracy of rainfall estimation. Temporal errors (graphs of ME versus time) indicate the temporal estimate errors and generally showed that the overestimated very small rainfall values and reversed to underestimate for heavy rainfall in both areas. 3B42 V7 has relatively less MAE value in low elevation grid area but 3B42RT in high elevation. The value of MAE is keeping increasing from 3hour to 12 hour but its value suddenly fall down at daily rainfall to its minimum. Fig_13 and Fig_14, show the characteristics of satellite rainfall estimate errors with different temporal rainfall. Though maximum and minimum values vary with time scale, the satellites overestimated very small rain rates and underestimated heavy observed rainfalls in both areas. The errors vary from +3 times the minimum rainfall value to -0.67 times of that maximum value. Again, of the total 3hourly estimations 85% of 3B42 V7, 82 % of 3B42RT and 64% for

CMORPH (low elevation area) and 81% for 3B42RT, 71% for 3B42V7, and 67% for CMORPH (high elevation area) were within 3hour maximum and minimum observed values. Percentage of estimate values which lay between minimum-maximum observed values (Appendix II: Table 2 & 3). The lesser the value shows the rest number of estimations were for sure overestimated or underestimated the actual rainfall. Here, we learned that to obtain estimates in the range of maximum and minimum rain gauge (RG) value, the 3hour and 6hour estimates are more preferable.

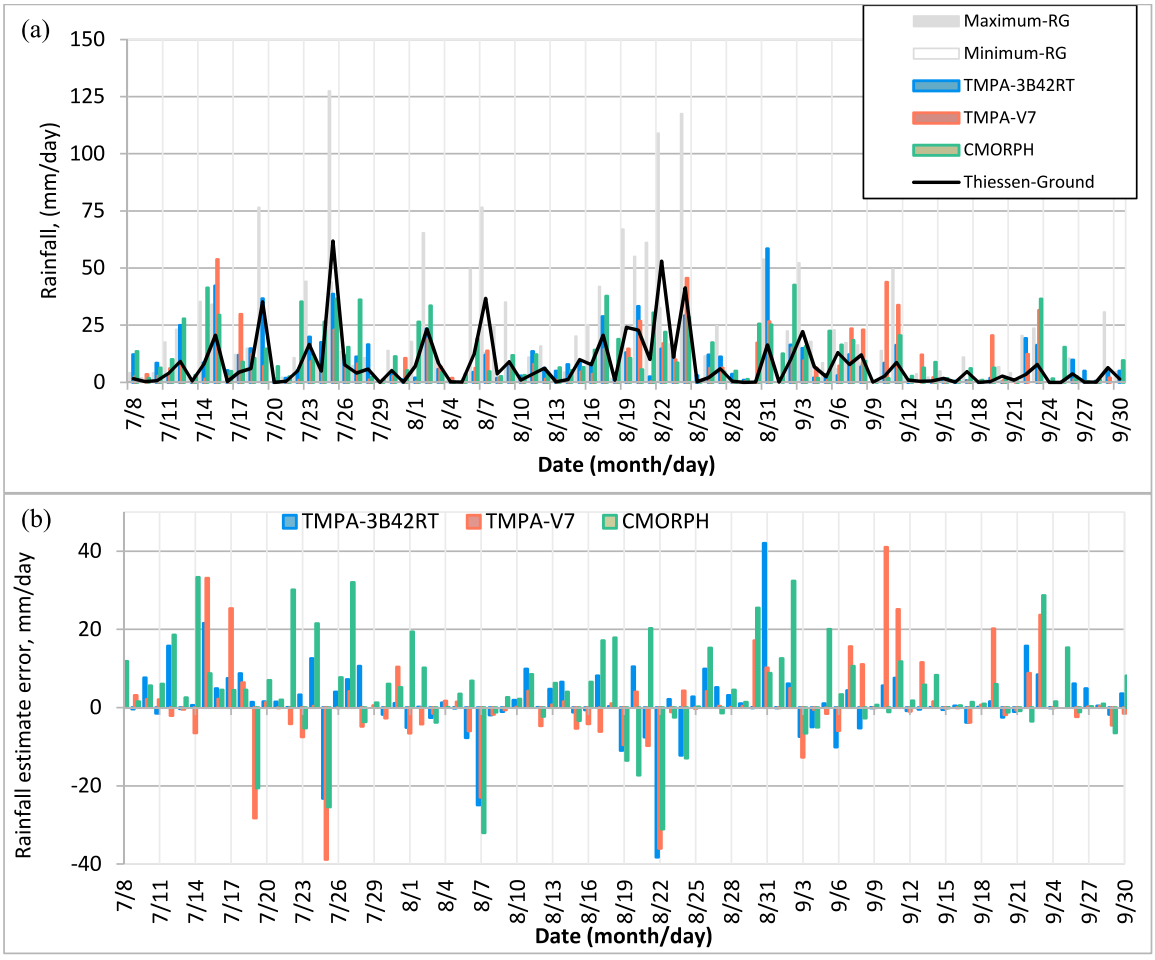

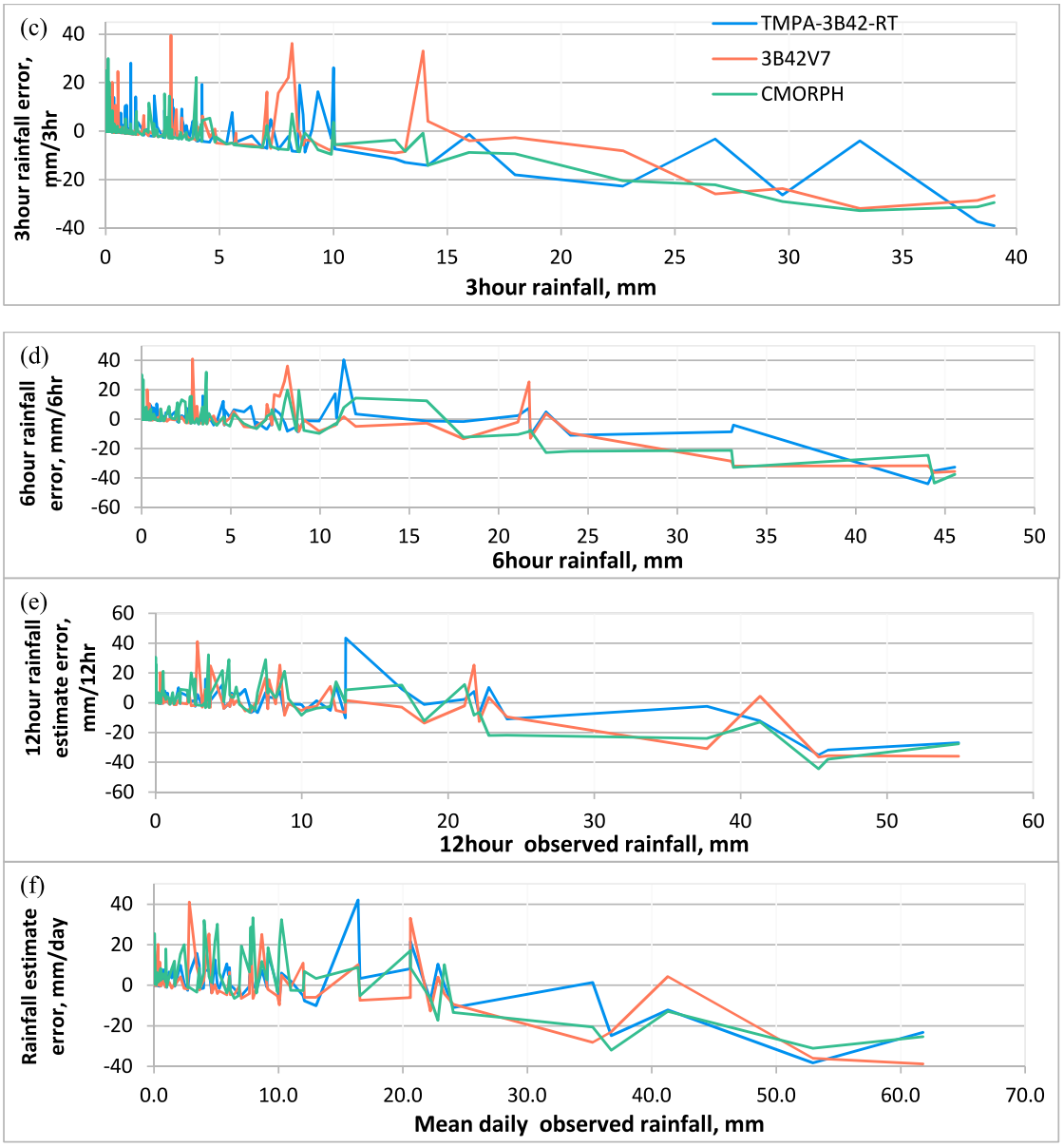

Figure 13: Graphs of rainfall observations in low elevation. (a) Daily rainfall of ground and three estimates. (b) Daily estimate error of the estimates and (c through f) error as a function of mean observed rainfall at different time scale.

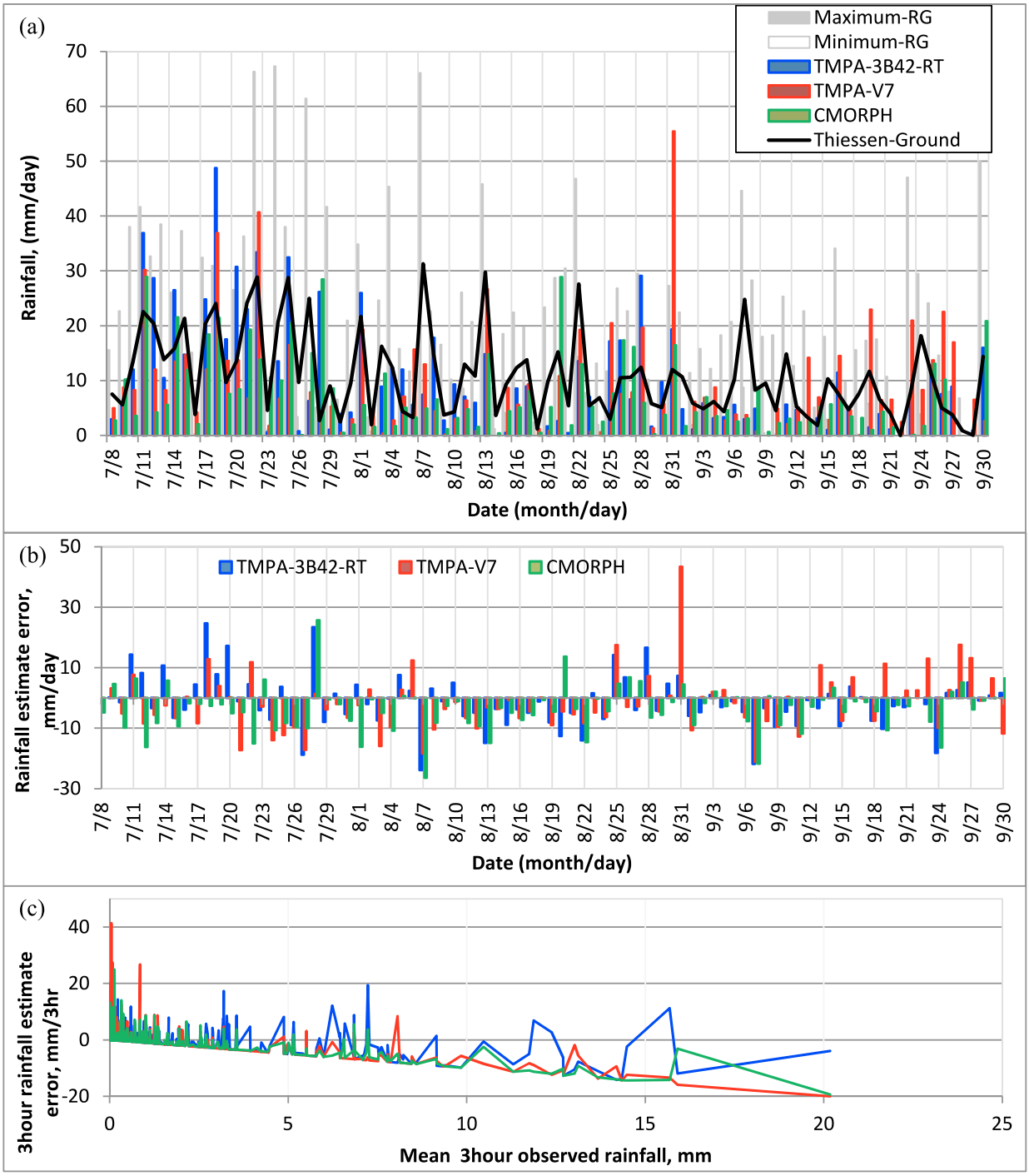
(a)
Maximum-RG
Minimum-RG
TMPA-3B42-RT
TMPA-V7
CMORPH
Thiessen-Ground
Rainfall, (mm/day)
Date (month/day)
(b)
TMPA-3B42-RT
TMPA-V7
CMORPH
Rainfall estimate error, mm/day
Date (month/day)
(c)
3hour rainfall estimate error, mm/3hr
Mean 3hour observed rainfall, mm

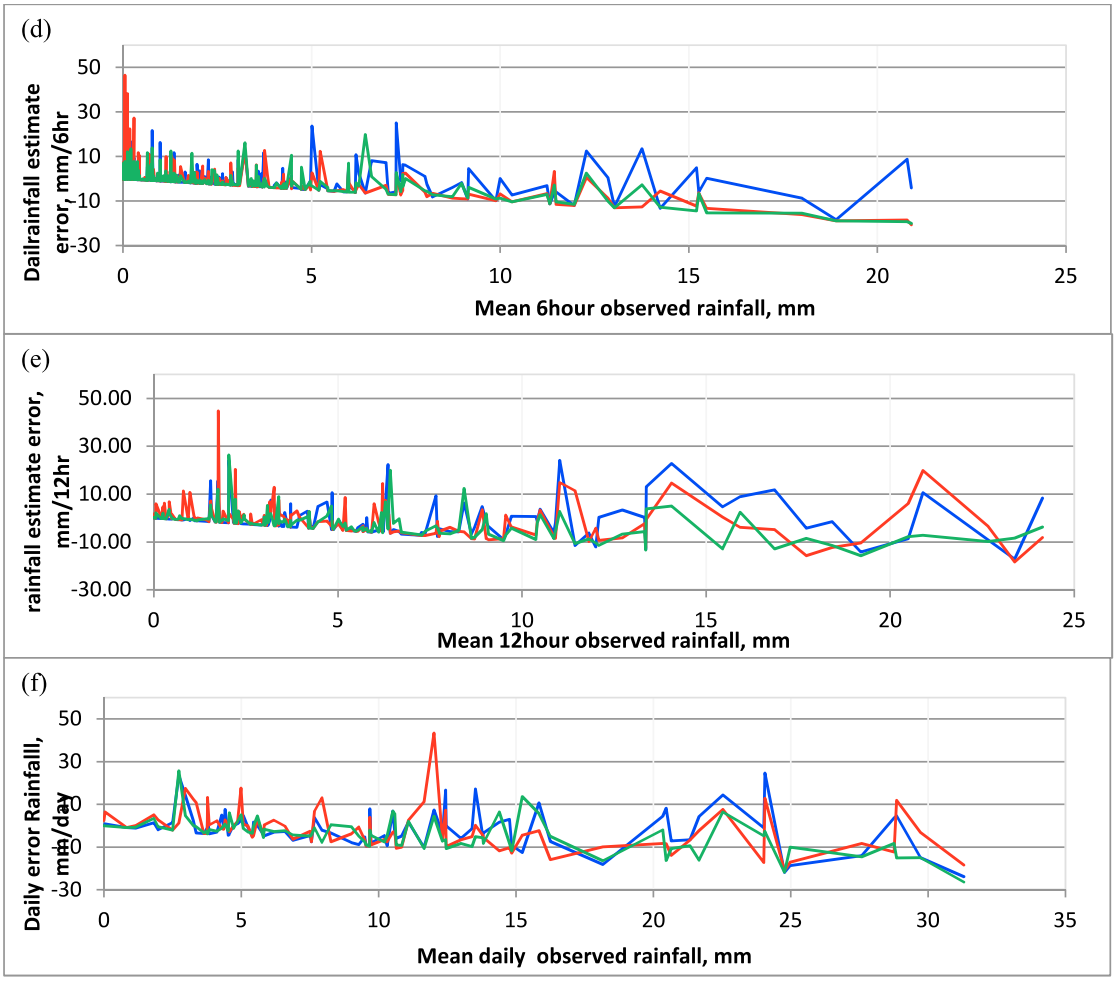

Figure 14: Graphs of rainfall observations in high elevation. (a) Daily rainfall of ground and three estimates, (b) Daily estimate error of the estimates and (c through f) error as a function of mean observed rainfall at different time scale.

In addition to the standard statistical rainfall value error measures, the estimates were also verified using categorical statistics at those temporal scales. They include probability of detection (POD), false alarm ratio (FAR), critical success index (CSI) and hanssens and kuipers discriminate (HK). These parameters show the performance of detecting the occurrence of rainfall (identifying rain-no rain) event but not the amount of rainfall. The rain no-rain threshold used for the contingency table is greater than 0.00 mm for all temporal scales. Values of these parameters significantly vary with changing the temporal resolution

from 3hour to daily in both areas. In both areas, the three rainfall estimates become more accurate at daily observation. So, it is important to see and evaluate these parameters at fine temporal resolution. In low elevation (Fig_15), there is difference between the products in detecting the rainfall events. POD value indicates fraction of estimated events which correspond to the observed rainfall events. CMORPH has the best potential of detecting raining clouds than the others. This value increased with time interval (example. CMORPH: from 3hr = 0.7 to daily = 1.0). So, at all time scales, CMORPH has best skill and both the TMPAs have equal POD value of 0.5 for 3hour data. While, TRMM 3B42-RT has less false alarm ratio (with FAR = 0.2 for 3hourly) during the study period at all time scales except at daily scale. CMORPH had high number of non-rainy detected events. All the products have same converged FAR value of about 0.00 at daily time scale. CSI better indicator than POD because it includes the three (hits, false alarms and miss) events, though like POD it does not distinguish source of estimate error. Fig_15 (c) show CMORPH highly affected by miss estimates from the change POD value to due to the inclusion of miss events.

The HK discriminate indicates accuracy of an estimate to separate rain events from non-rain events with perfect score of 1.0 (for estimate having only hits), -1.0 (for estimate having only false alarm); and zero for no skill. Therefore, Fig_15 (d), TMPA 3B42 RT and V7 products show better event matching with the observed in increasing slope with time scale till 12hour (HK = 0.4 and 0.3 respectively at 3hour). But HK = 0.2 at 3hour estimates from CMORPH were matched with observed. All the rainfall estimates recorded more events than the actual observed events at all temporal resolutions.

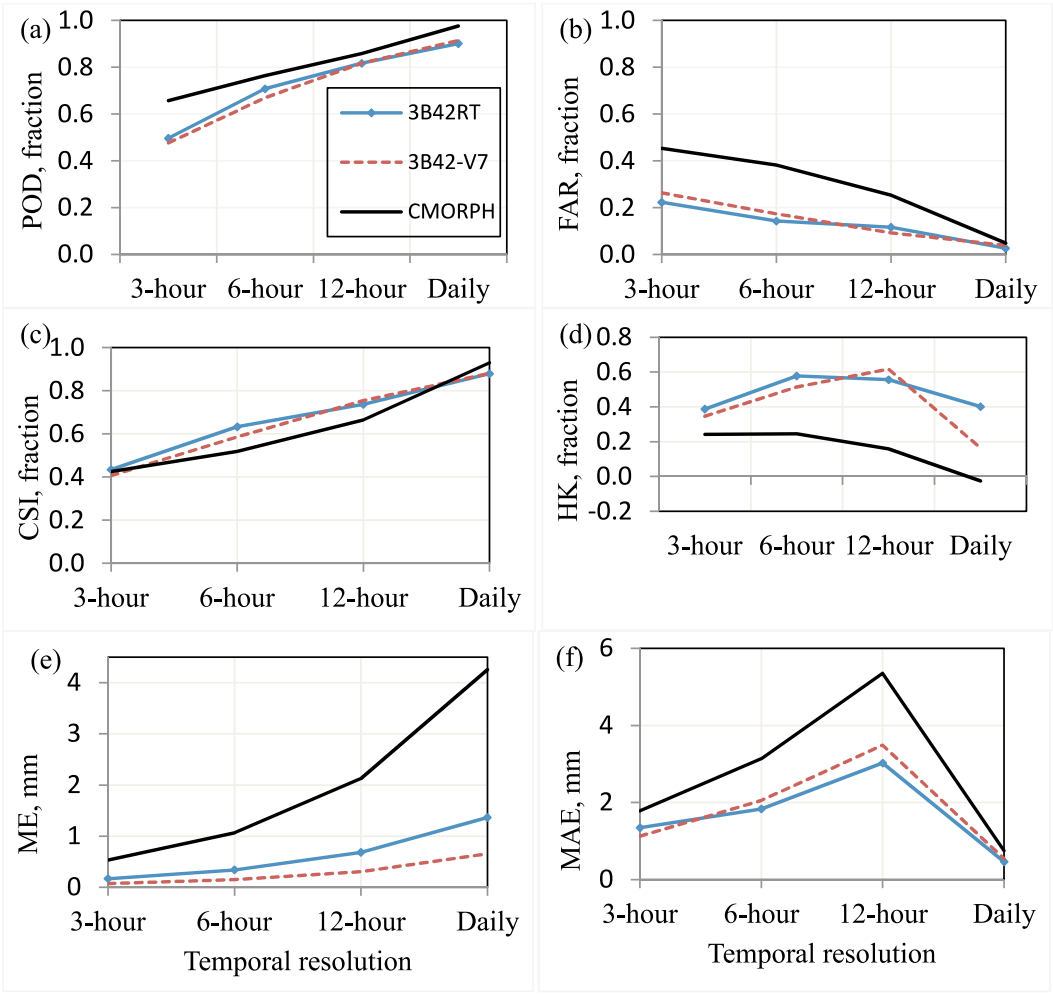

Figure 15: Verification measures of satellite estimates (low elevation area): (a) POD, (b) FAR, (c) CSI, (d) HK, (e) mean error, and (f) mean absolute error.

Fig_16 represented the categorical statistical measures of the rainfall estimates accuracy in the high elevation area. CMORPH has best ability of rainfall detection in comparison the TMPA 3B42 satellite products with POD of 0.6 and 1.0 (3hour and daily respectively) values. The rain event detection ability of this product showed best capturing the actual rainfall regardless of volume ratio. Based on 3hour temporal scale, both TMPA estimates have similar

POD value which is equal to 0.3. FAR for 3B42RT (varying from 0.1 (3hourly) to 0.0 (daily)) indicating rainfall event estimate from this product has less false alarm ratio (0.1).

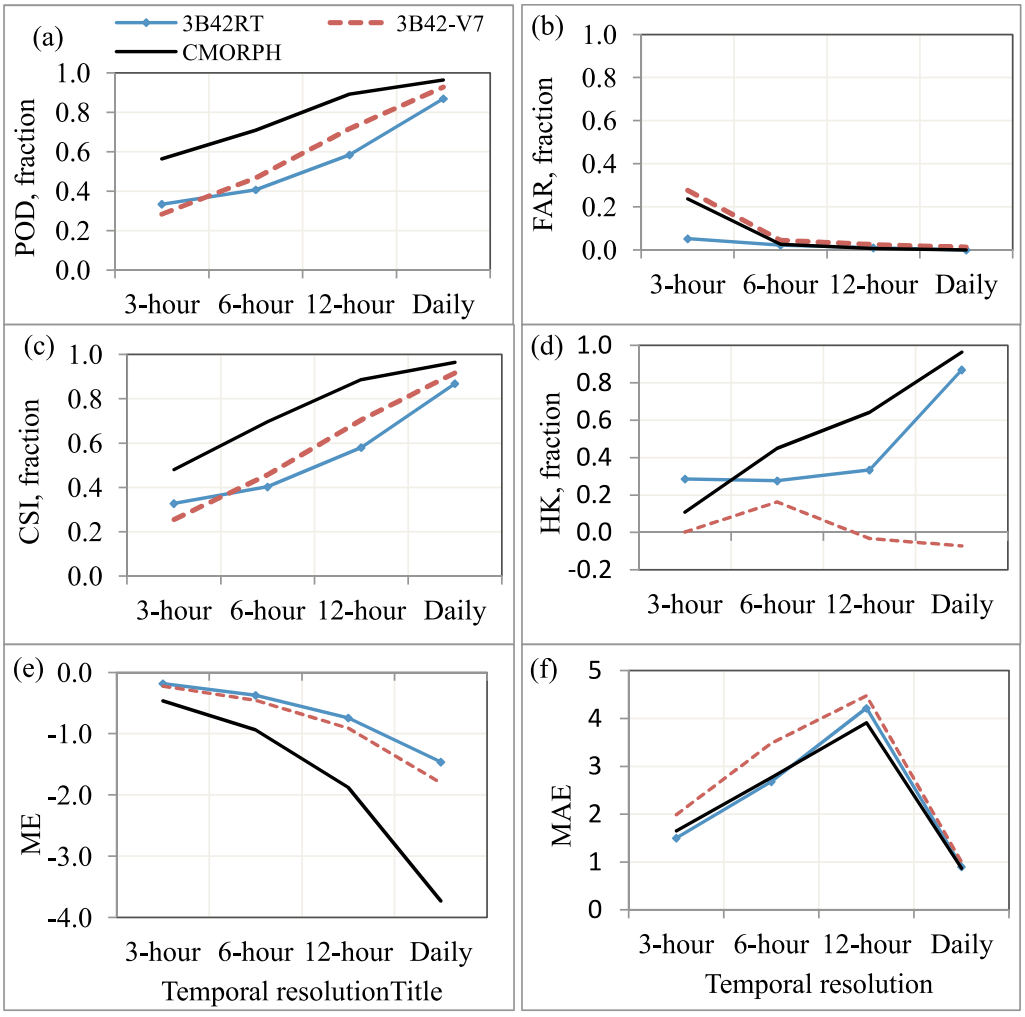

Figure 16: Verification measures of satellite estimates (high elevation area): (a) POD, (b) FAR, (c) CSI, (d) HK, (e) mean error, and (f) mean absolute error.

At 3hour estimates, CMORPH and TMPA 3B42 V7 were influenced by estimating more non rainy clouds. The product with higher FAR (0.3) is TRMM 3B42-V7.

All satellite estimates significantly affected by the miss estimate values specially CMORPH which performed well in detecting less false alarms. The CSI value of 3hour and daily varied from 0.3 to 1.0 for CMORPH, 0.3 to 0.9 for TMPA 3B42 V7 and 0.3 to 0.9 for TMPA 3B42

RT. This influence decreased with increasing time scale. CMORPH and TRMM 3B42 RT had better skill to separate (HK) rain cases from non rain estimates which increasing with time interval. Increasing positive value of HK for CMORPH and TRMM 3B42 RT indicating more daily events were corresponding with observed events; but, TRMM 3B42 V7 has less skill to separate the rain and non rain cases with HK = 0.0 and 3B42 RT has better HK; 0.3 at 3hour.

4.5 Effect of Elevation on Local Scale Rainfall Distribution

The local scale rainfall distribution was analysed based on different statistical measures including spatial coefficient of variation. As, discussed in previous sections rainfall generally has a random characteristics in the low elevation area. Whereas, the variability has a relation to elevation difference; that is the higher the point is frequent and high seasonal accumulated rainfall. We also considered deviation of daily observations from their spatial mean rainfall. Spatial mean rainfall values which contributed for the 75% of the total seasonal were considered. Reason is small rain rate yields very large CVt and these are not more important in any applications or decision making. For this analysis daily data was used to assess Sub-grid rainfall distribution. We consider three (maximum, median and minimum) CVt values. Here, in Table_.4 shown the sub grid spatial rainfall variability.

Table 5: Spatial daily coefficient of variation on three selected daily observations between rain gauge stations in the two grids.

a.	**Station Code_Name (Low elevation grid)**								
Date	40_ Rdam	41_ Alemayehu	42_ abujar	43_ Yabulu	44_ Abraham	45_ Yetzig	47_ Nasir	48_ Jalot	Mean
i.	For the minimum daily CVt value ~ 17%								
8/3/12	-	10.2	12	9	7	8	9	8	8.2
Ri-$\bar{R}$d	-	2	4.2	1	-1.2	-0.2	0.8	-0.2	
%	-	24	51	12	-15	-2	10	2	
ii.	For the mediann daily CVt value ~ 77%								
7/12/12	-	23	15	14	7	9	10	0.3	9.2

Ri-$\bar{R}$d	-	14	5.8	4.8	-2.2	-0.2	0.8	-8.9	
%	-	150	63	52	-24	-2	9	-97	
iii.	For the largest daily CVt value ~ 210%								
8/21/12	1	9	16	2	12	61	3	1	10
Ri-$\bar{R}$t	-9	-1	6	-8	2	51	-7	-9	
%	-90	-10	60	-80	20	510	-70	-90	

b.	**Station Code_Name (High elevation grid)**									
Date	24_ Atiha	25_Genet abo	26_ Maksegnit	27_ Amistegna	29_ Ajale	31_ Dangber	33_ Bahta	34_ senebo	38_Leba gedel	Mean
i.	For the minimum daily CVt value ~ 15%									
7/18/12	31	27	25	22	20.2	19.8	25	25	22	24
Ri-$\bar{R}$d	7	3	01	-2	-4	-4	1	1	-2	
%	29	11	4	-9	-16	-18	3	3	-9	
ii.	For the median daily CVt value ~ 47%									
9/15/12	9.5	7.3	9.8	6.3	2.9	6.6	18	11	11.7	10
Ri-$\bar{R}$d	-0.5	-2.7	-0.2	-3.7	-7.1	-3.4	8	1	1.7	
%	-5	-27	-2	-37	-71	-34	80	100	170	
iii.	For the largest daily CVt value ~ 127%									
8/4/12	5.4	12.4	3	3	18.5	1.5	45.4	9.3	1.7	12
Ri-$\bar{R}$d	-6.6	0.4	-9	-9	6.5	-10.5	33.4	-2.7	-10.3	
%	-55	3.3	-75	-75	54	-87	278	-22	-85	

Table_4 (A), daily observation with minimum CVt (17%) in the low land area, the individual deviation from the spatial mean daily rainfall (~8.2mm) varied from -15% (gauge-44) to 51%(gauge-42). In July 12nd, with daily spatial mean of 9.2mm and CVt of 77%, gauge stations varied from -97% gauge 48 to 150% gauge 42. In August 21st event (with CVt = 210%) the deviation from the mean (mean=10mm) from -90% (gauge 48) to 510% gauge 45. And section (b) of Table (for high elevation) daily observation with less CVt (15%) the individual deviation from the spatial mean daily rainfall (~24mm) varied from -18% (gauge 31) to 29% (gauge 24). In Sep. 15th, with daily spatial mean of 10mm and median CVt value of 47%, gauge stations varied from -71% gauge 29 to 170% gauge38. In August 4th event

(with CVt=127%) the deviation from the mean (mean=12mm) from -87% (gauge 31) to 278% gauge 33.

The sub grid variability has not clear relation with the point elevation. It showed random characteristics of rainfall in both areas. But, sub-grid variability is higher at low elevation according to the daily minimum, median and maximum CVt values. For example, the daily median CVt inter-gauge deviation ranges for a magnitude of 260% and 240% in low elevation and high elevation area respectively. On these days daily mean rainfall was 9.2mm (low elevation) and 10mm (high elevation). Therefore, there is high local spatial rainfall variability in the low elevation grid. Indicating that, there is significant randomness property of rainfall in low elevation grid area.

In low elevation area spatial variability has random property and has no relation with elevation difference among gauge stations. But in high elevation grid, spatial CVt does have relation with elevation difference. For example, Ajale (elev. = 2613m) station over estimated by 54% the daily spatial reference rainfall and Dangber (elev. = 2067m) underestimated the spatial mean value by -87% on 4th of August.

4.6 Effect of Elevation on Accuracy of Satellite Rainfall Products

Using the spatial mean rainfall calculated using thiessen polygon method from the rain gauges within each grid area, three products were evaluated. The comparison was done based on both rainfall value and rainfall event detection ability. From the graphs of temporal error and error versus mean observed rainfall (Fig_13 and 14 and Appendix I: Fig_3), one can see the error estimate in the high elevation are less sensitive to extreme event values. In deeded, maximum rain events were highly underestimated in the low elevation area. When we look the ME and Bias from (Fig_ 15 and _16), mean estimated rainfall value are positively biased for all; 3B42 RT, 3B42 V7 and CMORPH in low elevation while all underestimated in high elevation grid. Elevation increment showed a change from positively bias to negative bias on rainfall amount estimation. In comparison the two grids, the three rainfall estimates were influenced by miss estimates in high elevation than low elevation. TMPA V7 is better in low elevation in terms of

ME, MAE and bias than the other two estimates. It is also less influenced by detecting non raining clouds or false alarms. In rainfall event estimate from TMPA RT had less bias (bias of 10%) and less false alarm ratio (FAR = 0.2) in low elevation.

In high elevation area 3B42RT has smaller ME, MAE, Bias, FAR and greater HK. Results in this site show the products are affected by miss observed rainfall events than in low elevation area. (Appendix II: Table 2 and 3) of 3hour rainfall estimates in the low land area, TMPA 3B42 RT (82%), TMPA 3B42 V7 (85%) and CMORPHP (64%) were within the range of minimum and maximum observed value. Correspondingly, TMPA 3B42 RT (81%), TMPA 3B42 V7 (71%) and CMORPHP (68%) were in the high elevation grid.

Generally, the results showed that; (a) 3B42V7 is preferable in the low elevation area and 3B42RT is best estimate in the high elevation area. (b) the estimates are affected by more miss estimates in high elevation than low elevation; see Appendix I: Fig_5. (c) the products are less affected by false alarm estimates in the high elevation than low elevation. (d) the products underestimated the actual rainfall in high elevation unlike in low elevation where they overestimate the actual rainfall.

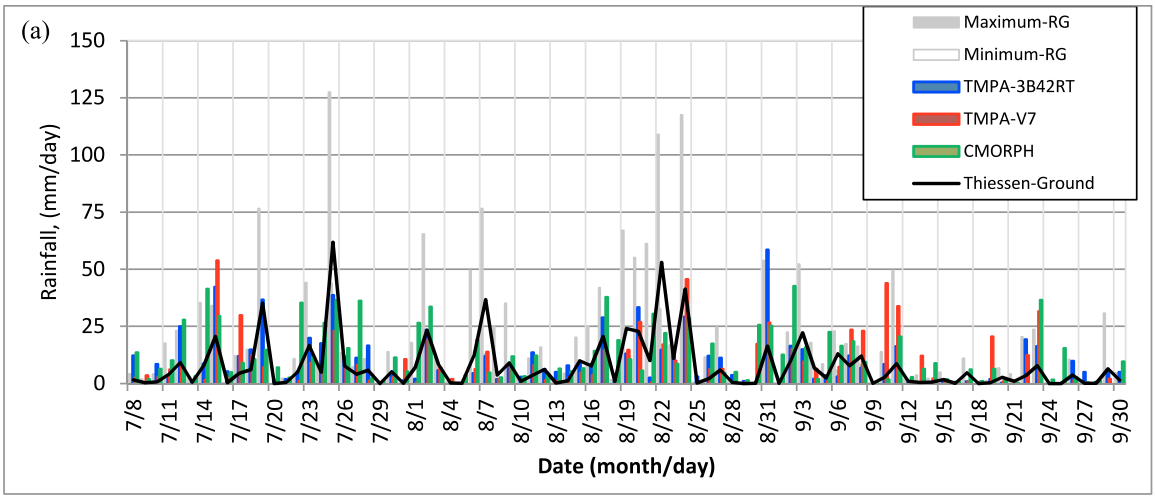

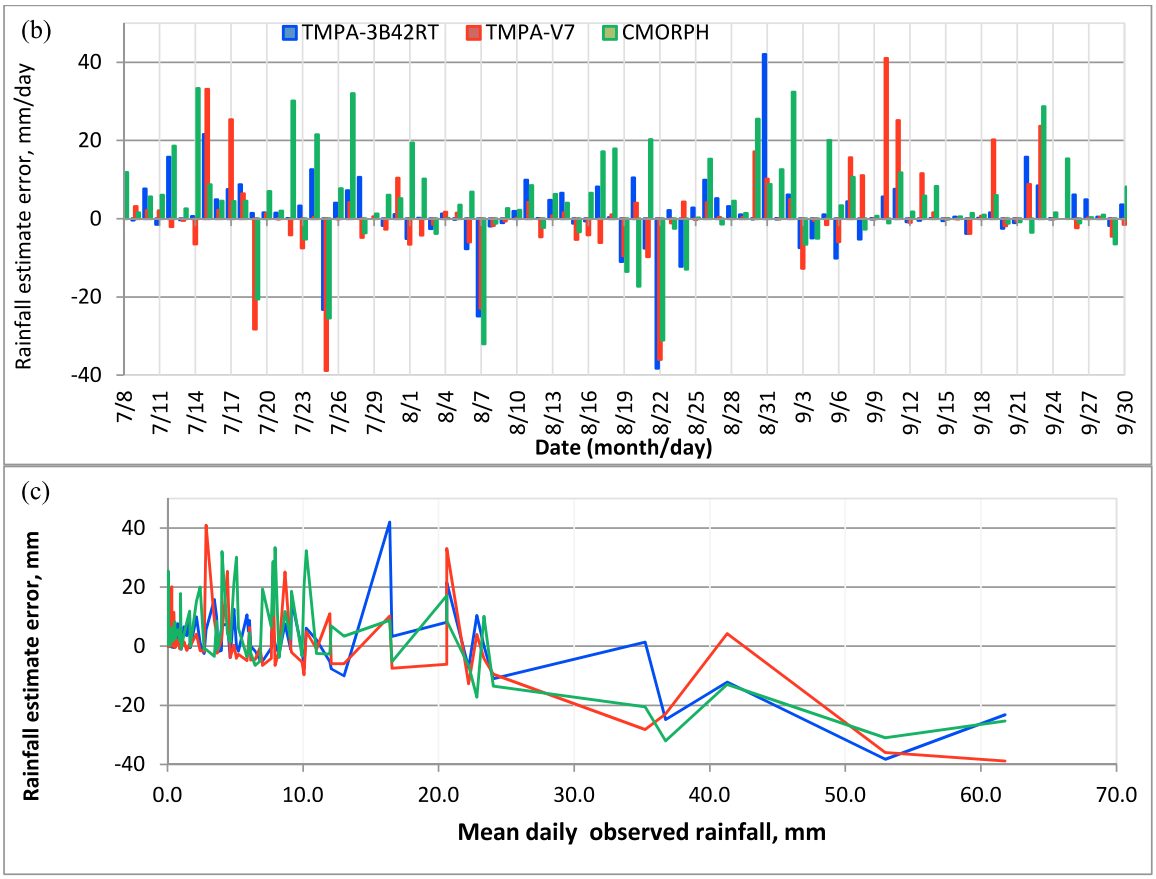

Figure 17: Graphs of rainfall observations in low elevation. (a) Daily rainfall of ground and three estimates. (b) Daily estimate error of the estimates and (c) error as a function of mean observed daily rainfall.

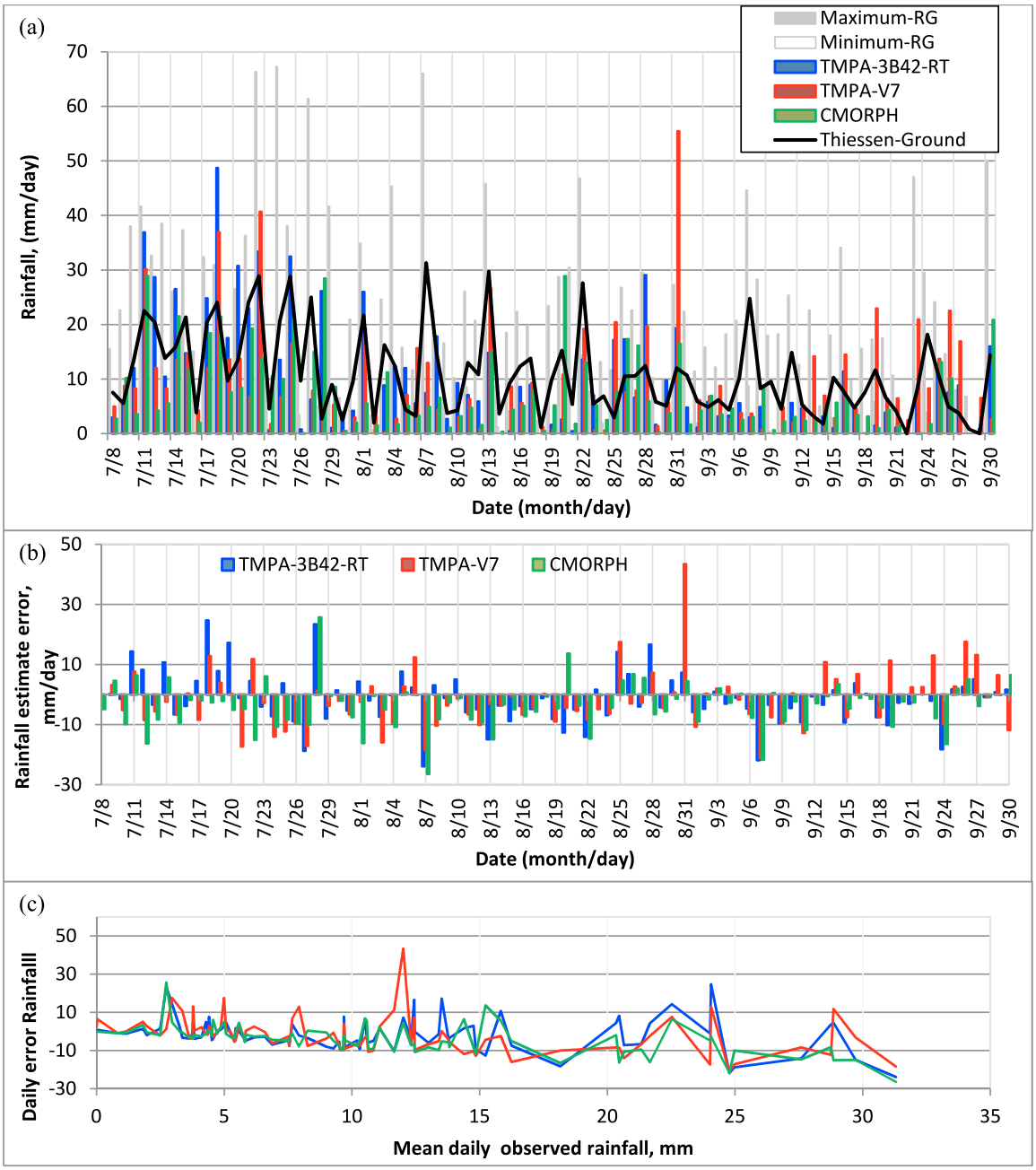

Figure 18: Graphs of rainfall observations in high elevation. (a) Daily rainfall of ground and three estimates, (b) Daily estimate error of the estimates and (c) error as a function of mean observed daily rainfall.

5. CONCLUSION AND RECOMMENDATIONS

5.1 Conclusions

In this study, we aim to assess rainfall characteristics such as; spatial-temporal rainfall variability and rain event properties. Effect of elevation on accuracy of three satellite rainfall estimates based on ground truth data across two contrasting elevation (25km x 25km) grid areas was analyzed. Standard statistical and categorical verification measures were used. Data was used from dense deployed automatic rain gauges in the Blue Nile Basin and from three remote sensed rainfall estimates for the study period from July 08 to Sep. 30, 2012 (85 days).

The temporal rainfall variability is significant in the low elevation area due to less rainy hours or rare rainfall events. Mean rainfall of low elevation varied from 629 mm to 969 mm while from 633mm to 1208mm in the high elevation area. There were 75mm and 30mm maximum daily rain rates in low and high elevation grids respectively. Low elevation had smaller total seasonal rainfall, smaller temporal mean rainfall depth and greater conditional mean rainfall. Percent of raining hours in high elevation varied between 6.4% and 13.8% while in the low elevation varied from 6.7% to 7.3% of the total hours of the analysis period. Both the smaller conditional mean rainfall and larger percent of rainfall duration show frequent hourly rainfall.

Diurnal cycle of low elevation has two sharp peaks at late night (0200 LST) with 1.9 and at the afternoon and early evening at 1700 with 1.3. High elevation has two peaks at 1700 LST with 1.5 standardized value of rainfall. Rainfall occurs during the whole times of the day in high elevation grid. Temporal coefficient of variation was significantly varied (decreased) in low elevation as temporal resolution become coarser. This shows, there were more alternatively driest and wettest rainfalls in the low elevation area. In both sites most dependable (representative) rainfall occurs at daily scale although precision differs.

High elevation area has more rain events (varying from 91 to 105) than low elevation (range 66 to 75) using MIT of 6hour dry time. Maximum event rain rate was 122mm/hour and 67mm/hour in low elevation and high elevation respectively. Unlike in low elevation area, there is significant correlation between distance and rainfall in high elevation. Gauges separated by 5km correlated with CC of 0.80 in high elevation and by 8km in low elevation

area with correlated by 0.75. Therefore, care should be taken in design of rain gauge network depending on the elevation of the area under interest.

The 3hour satellite rainfall estimates; 3B42RT, 3B42V7 and CMORPH (with biased of 20% and 10% and 50% respectively) overestimated the mean observed rainfall in the low elevation. In the contrary, 3B42RT, 3B42V7 and CMORPH underestimated the actual rainfall by 10%, 20%, and 30% respectively in high elevation area. In both sites, the products underestimated 3hourly and 6hourly maximum rainfall observations by about 50%. CMORPH is best in detecting (POD), in both area but it was influenced by false alarms in low elevation and by misses in high elevation area. TMPA V7 has performed better in low elevation in terms of POD, CSI and bias than in high elevation. Rainfall event estimate from TMPA RT had less bias and less false alarm ratio (FAR = 0.2) in low elevation.

A rainfall estimate with the order of less mean error (bias), less absolute error, high critical success index, high probability of detection, and less false alarm ratio is thought to be preferable. The reason is bias (volume ratio) and mean error (difference) measure in relation to the actual rainfall amounts. 3B42V7 has better performance followed by 3B42 RT in estimating the actual rainfall value in low elevation. 3B42RT is best in high elevation grid area followed by 3B42 V7.
Generally, the results showed that the products;

(**i**). when terrain elevation increases the overestimation reversed to underestimation the actual rainfall (**ii**). are less affected by false alarm estimates in the low elevation than high elevation. (**iii**). are affected by more miss estimates in high elevation than low elevation. (**iv**). height of cloud has an influence on the satellite rainfall estimate. For example; the actual cloud height in high elevation is smaller than its apparent height because of cloud process due to topography. (**v**). CMORPH estimate is worst rainfall estimate in both sites but comparatively better in high elevation area.

5.2 Recommendations

The following recommendations are potential inputs for similar and related research works planned to be done in the future.

Quality of data being used for the purpose of validation has greater influence than the errors occur in the satellite estimation. Therefore, should be checked especially when it is based on the existing data unlike this study. Remotely sensed rainfall estimation data are potentials especially due to their temporal and spatial coverage. But, they need to be validated for the region of interest using qualified ground truth data.

This study was limited for the rainy season period of the area from July 8 – Sep. 30, 2012. The seasonal rainfall of the two areas during the analysis time was ranging from 633mm to 1010mm (except one rain gauge which received 1208mm) which is below the average annual rainfall (which is 1100mm) of the areas. Therefore, result of this work will be effective in this time interval with rainfall below the annual average rainfall or the drier raining season.

Most of the studies conducted in Upper Blue Nile have been targeted on the high elevation part of the basin. Therefore, as topography plays a great role on nature of rainfall properties, more studies should be needed especially in low elevation portion.

Accuracy of satellite rainfall estimates radically changed from region to region and depending on elevation. Therefore, the fine resolution satellite rainfall products evaluated in this paper and others should be verified for the area of interest.

6. REFERENCES

Cohen T. Liechti, J. P. Matos, J. L., Boillat and A. J. Schleiss, 2011: Comparison and evaluation of satellite derived precipitation products for hydrological modeling of the Zambezi River Basin; Jour. Hydrology and Earth Sys. Sci. Discussions: 8, 8173-8201.

Gebremichael M. and T. G. Romilly, 2011. Evaluation of satellite rainfall estimates over Ethiopian river basins. Journal of Hydro. and Earth System Sciences. 15, 1505–1514.

Haile A. T., T. H. M. Rientjes, , E. Habib, V. Jetten, , and M. Gebremichael , 2011: Rain event properties at the source of the Blue Nile River. Hydrol. Earth Syst. Sci., 15, 1023–1034.

Hong, Y., K. L. Hsu, S. Sorooshian, and X. Gao, 2004: Precipitation Estimation from Remotely Sensed Imagery Using an Artificial Neural Network Cloud Classification System. *J. Appl. Meteor.*, 43, 1834–1852.

Huffman, G. J., and Coauthors, 2007: The TRMM Multi-satellite Precipitation Analysis (TMPA): Quasi-global, multiyear, combined-sensor precipitation estimates at fine scales. J. Hydrometeor., 8, 38–55.

Joyce, R. L., J. E. Janowiak, P. A. Arkin, and P. Xie, 2004: CMORPH: A method that produces global precipitation estimates from passive microwave and infrared data at high spatial and temporal resolution. J. Hydrometeor., 5, 487–503.

Kummerow, C., W. S. Olson, and L. Giglio, 1996: A simplified scheme for obtaining precipitation and vertical hydrometeor profiles from passive microwave sensors. IEEE Trans. Geosciences Remote Sensing, 34, 1213–1232.

Mason, I. B., 2003: Binary events.Forecast Verification—A Practitioner's Guide in Atmospheric Science, I. T. Jolliffe and D. B. Ste-phenson, Eds., Wiley, 37–76.

McCuen, R.H., 1998: Hydrologic Analysis and Design. 2nd ed, Prentice Hall, Englewood Cliffs, NJ.

Menberu Meles and Mekonnen Gebremichael, 2008. Evaluation through independent measurements: Complex terrain and humid tropical region in Ethiopia. In Satellite Rainfall Applications for Surface Hydrology, M. Gebremichael and F. Hossain, Eds., Springer-Verlag. Springer Dordrecht Heidelberg London New York.

Menberu M., Mekonnen G., F.Y., Hirpa, Y . Michael, Y. seleshi, and Y. Girm, 2008. On the Local-scale Spatial Variability of Daily Rainfall in the Highlands of the Blue Nile: Observational Evidence. J. Atmospheric research, xx-xxxx.

Nesbitt, S. W., D. J., Gochis and, T. J., Lang, 2008: The Diurnal Cycle of Clouds and Precipitation along the Sierra Madre Occidental Observed during NAME-2004: Implications for Warm Season Precipitation Estimation in Complex Terrain. J. Hydrometeo. 9(4), 728–743.

Reichardt, K., L.R.Angelocci, o.o.s.,Bacchi, J.E., Pilloto, 1995: Daily Rainfall Variability at a Local Scale, inPracicaba, SP, Brazil, and its Implications on Soil Water Recharge. Sci. agric., 52(1), 43-49

Tufa D., P. Ceccato and S. Connor, 2008: Evaluation of Satellite Rainfall Estimates and Gridded Rain gauge Products over the Upper Nile Region. International Research Institute for Climate and Society the Earth Institute at Columbia University.

Tobin, K. J., and E. M., Bennett, 2010: Adjusting Satellite Precipitation Data to Facilitate Hydrologic Modeling. J. hydrometeor., 11, 966-977.

Wilk, J., D. Kniveton, L. Andersson, R. Layberry, M. C. Todd, D. Hughes, S. Ringrose, and C. Vanderpost, 2006: Estimating rainfall and water balance over the Okavango River TOBIN Basin for hydrological application. J. Hydrol., 331, 18–29.

Wouter, B., C. Ronaldo, W. Patrick, B.D., Bert, 2006: Spatial and temporal rainfall variability in mountainous areas: A case study from the south Ecuadorian Andes. J. hydrol.., xxx, xxx-xxx.

Ymeti I., 2007. Rainfall Estimation by Remote Sensing for Conceptual Rainfall runoff Modeling in the Upper blue Nile basin: Master's Thesis. International Institute for Geo-information Science and Earth Observation Enschede, The Netherlands.

URL:http://tornado.sfsu.edu/geosciences/classes/m356/RainfallVariability/TemporalVariability (accessed on Dec. 7, 2012 at 01:30 Am)

7. APPENDIX

Appendix I: Figure

Figure 1: Field work campaign photos demonstrating field stay.

(a)

(b)

(c)

(a) Searching possible rain gauge station location; Shambel Habte, Dr. Menberu and Me; from left to right.

(b) During downloading the rain gauge data from the rain gauges and

(C) When the surface of the soil was being cleaning to avoid intervention of the grass for the accuracy of the instrument.

Figure 2: Schematic sketch of a typical rain gauge station and its distance from obstructions for a gauge station.

Latitude: 11.1292^0	Region: BenshangulGumuze	Equipment type: Automatic rain gauge
Longitude: 35.4672^0	Zone: Metekel	Station ID: 47
Elevation: 614m	Town: Wembera	Data type: Rainfall
Launched date: 26/06/2012	Keble: Nasir	Specific place: Beles
Distance from Addis Ababa: 893Km		

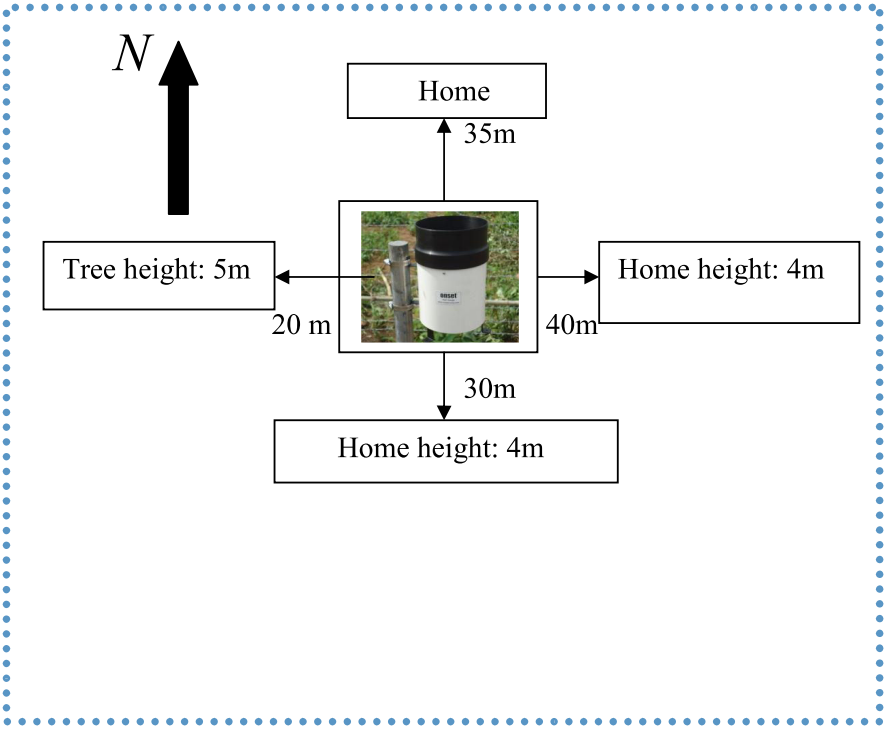

Photo: view - 1

Photo: view - 2

Figure 3: Temporal satellite rainfall estimate error for 3hour, 12hour and 12hour in the low elevation

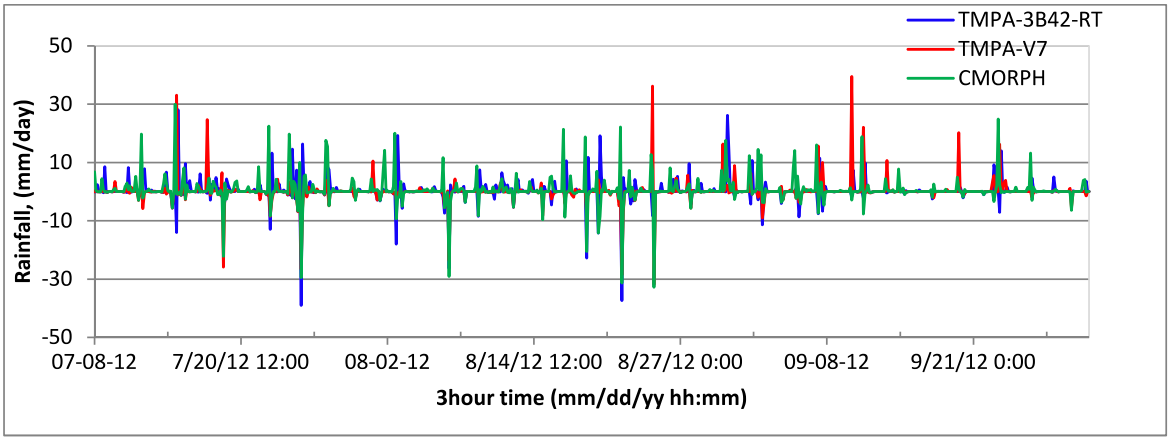

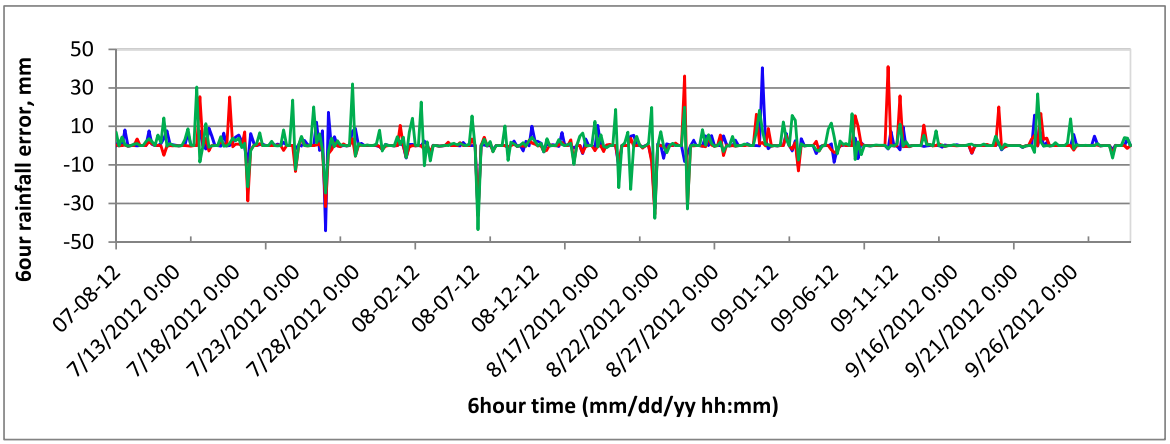

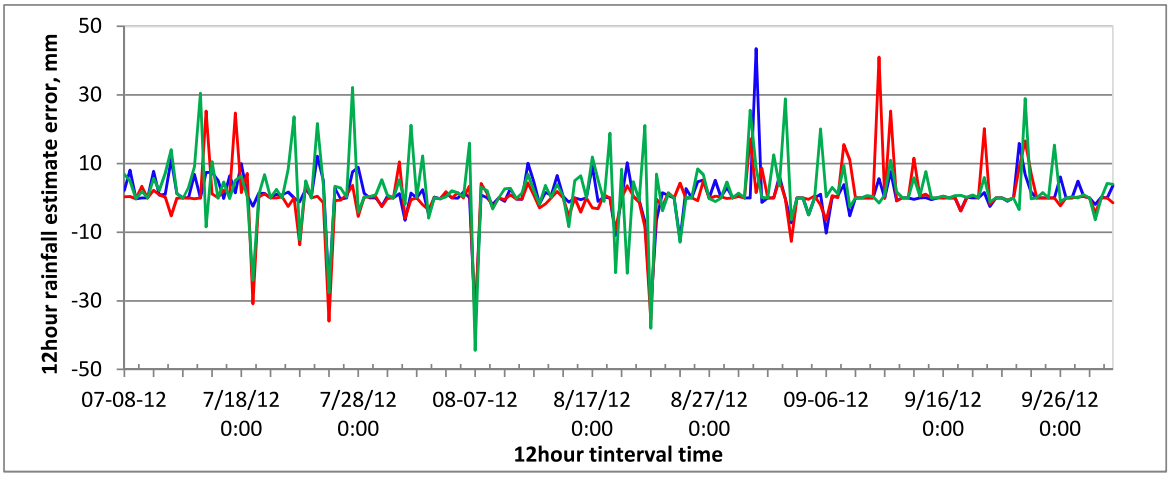

Figure 4: Temporal satellite rainfall estimate error for 3hour, 12hour and 12hour (down) respectively in the high elevation area.

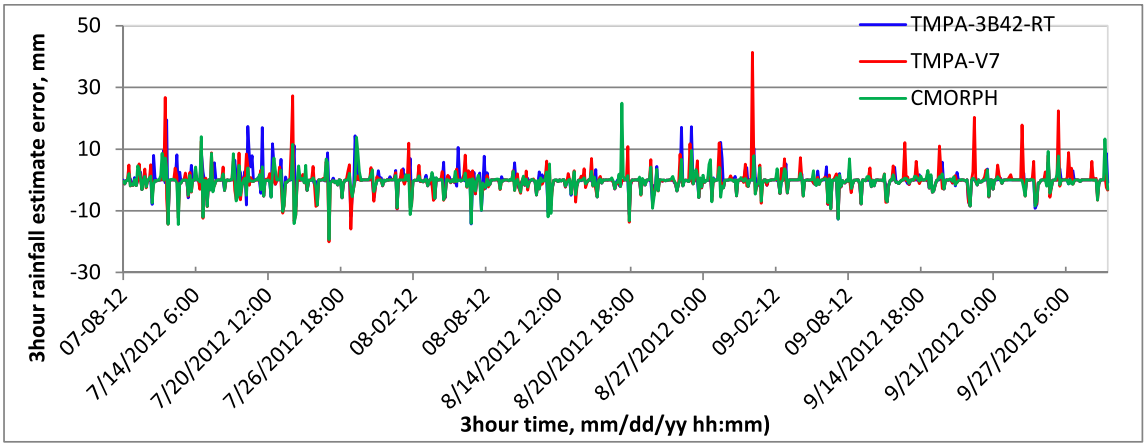

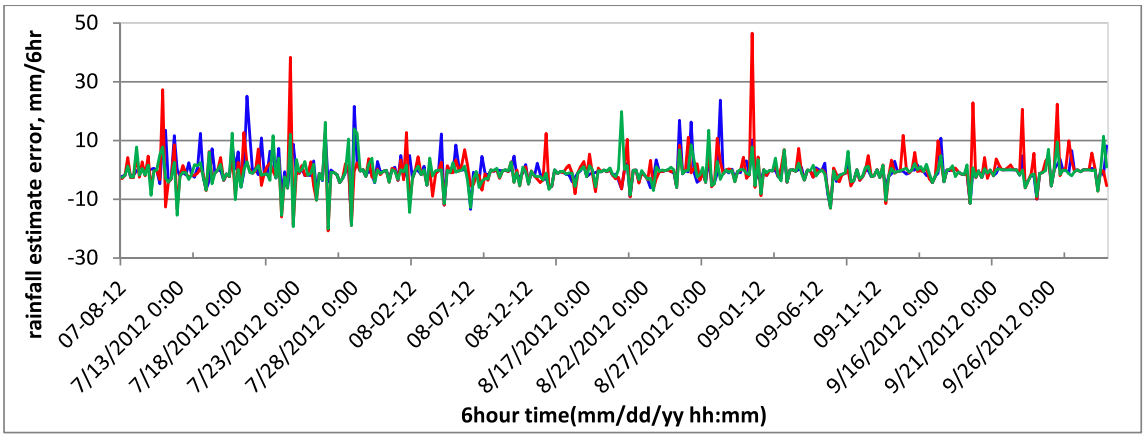

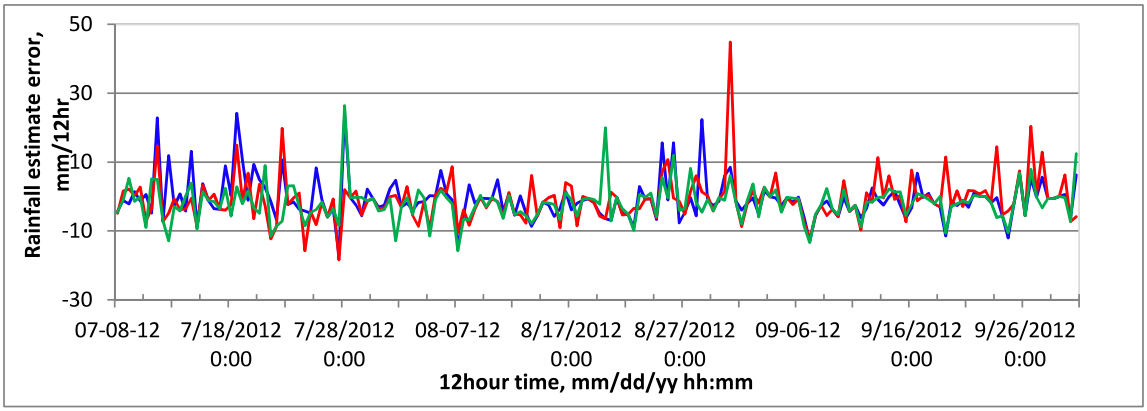

Figure 5: Values of the categorical verification measures of the three satellite rainfall estimates. Hits (A), False alarms (B), Misses (C) and Correct negative (D) depending on 3hour rainfall observation. The left column is for low elevation and right column is for high elevation area.

Low Elevation

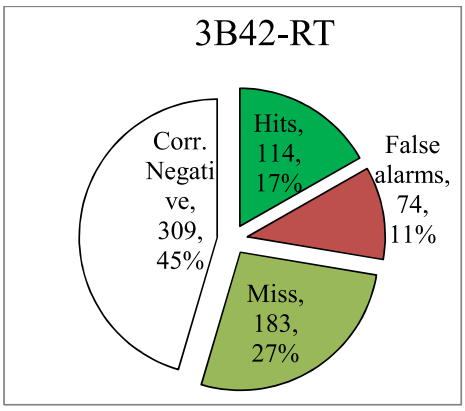

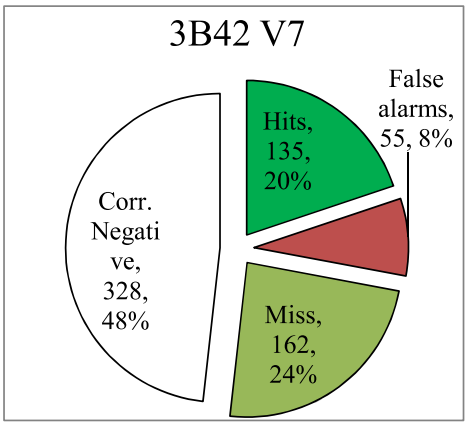

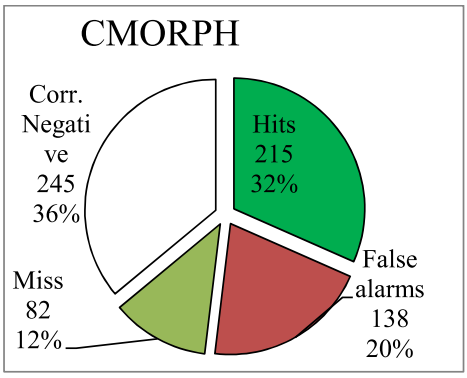

High Elevation

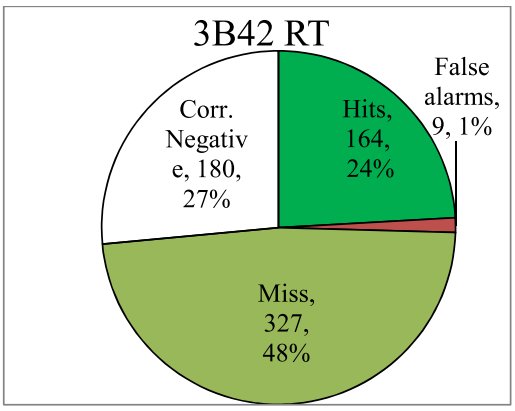

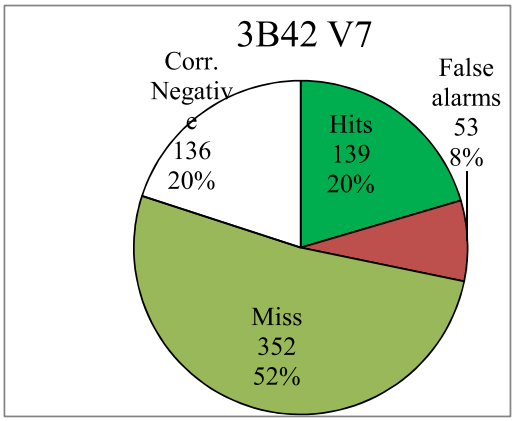

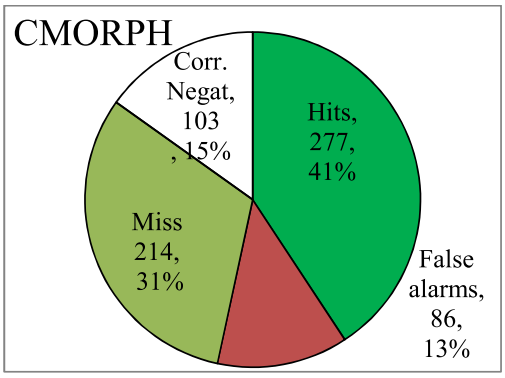

Appendix II: Table

Table 1: Data characteristics of satellite rainfall estimate products used.

	TRMM-TMPA		CMORPH
	3B42_RT	3B42_V7	CMORPH
Temporal coverage	Start Date: 1997-12-31 Stop date: -	Start Date: 1997-12-31 Stop date: -	Start Date: 2002-12-03 Stop date: -
Geographical coverage	Lat: 50°N-50°S; Lon: 180°W-180°E	Lat: 40°N-40°S; Lon: 180°W-180°E	Lat: 40°N-40°S; Lon: 180°W-180°E
Temporal resolution	3-Hourly	3-Hourly	3-Hourly
Data available after observation	6hour	2 to 3 months	22 to 44 hours
Spatial resolution	0.25°*0.25°; nlat = 400; nlon =1440	0.25°*0.25°; nlat = 320 nlon = 1440	0.25°*0.25°; nlat = 480 nlon = 1440
File Type	Binary	HDF	Comb.Z
Granule ID	3B42RT.yyyy.mm.dd.HHz.bin	3B42.yyyymmdd.HH.7.HDF.Z	yyymmdd_3hr-25deg_cpc+comb.z
CMORPH TMPA_3B42RT TMPA_3B42_V7	ftp://ftp.cpc.ncep.noaa.gov/precip/global_CMORPH/3-hourly_025deg/ ftp://disc2.nascom.nasa.gov/data/TRMM/Gridded/3B42RT http://mirador.gsfc.nasa.gov/cgi-bin/mirador/presentNavigation.pl?tree=project&dataset=3B42:3-our0.25x0.25degreemergedTRMMandothersatellite estimates& project= TRMM&dataGroup=Gridded&version=007		

Note: **nlat** : number of 0.25° latitude grids from 50°N - 50°S for RT; 40°N - 40°S for V7 and from 60°N - 60°S for CMORPH. **nlon** = 1440: number of 0.25° longitude grids from 180°W - 180°E of all the three; **Yyyy.mm.dd.TT** = year.month.day.time

Table 2: Results of statistical verification measures of the satellite rainfall estimates in low elevation area.

		3_hour_Low Elevation			6_hour_Low Elevation		
Notation	Statistics	3B42RT	3B42-V7	CMORPH	3B42RT	3B42-V7	CMORPH
POD	Probability of Detection	0.5	0.5	0.7	0.7	0.7	0.8
FAR	False Alarm Ratio	0.2	0.3	0.5	0.1	0.2	0.4
()	%	81.6	84.6	63.8	38.5	38.5	26.3
CSI	Critical Success Index	0.4	0.4	0.4	0.6	0.6	0.5
HK	Hanssen and Kuipers disc	0.4	0.3	0.2	0.6	0.5	0.2
Bias	Bias	1.2	1.1	1.5	1.2	1.1	1.5
ME	Mean error	0.2	0.1	0.5	0.3	0.2	1.1
MAE	Mean Absolute error	1.3	1.1	1.8	1.8	2.1	3.1

		12_hour_Low Elevation			Daily_Low Elevation		
Notation	Statistics	3B42RT	3B42-V7	CMORPH	3B42RT	3B42-V7	CMORPH
POD	Probability of Detection	0.8	0.8	0.9	0.9	0.9	1.0
FAR	False Alarm Ratio	0.1	0.1	0.3	0.0	0.0	0.0
()	%	16.3	16.9	10.9	61.2	64.7	43.5
CSI	Critical Success Index	0.7	0.8	0.7	0.9	0.9	0.9
HK	Hanssen and Kuipers disc	0.6	0.6	0.2	0.4	0.2	0.0
Bias	Bias	1.2	1.1	1.5	1.2	1.1	1.5
ME	Mean error	0.7	0.3	2.1	1.4	0.7	4.3
MAE	Mean Absolute error	3.0	3.5	5.4	0.5	0.5	0.8

Table 3: Results of statistical verification measures of the satellite rainfall estimates in high elevation area.

		3_hour_High Elevation			6_hour_High Elevation		
Notation	Statistics	3B42RT	3B42-V7	CMORPH	3B42RT	3B42-V7	CMORPH
POD	Probability of Detection	0.3	0.3	0.6	0.4	0.5	0.7
FAR	False Alarm Ratio	0.1	0.3	0.2	0.0	0.0	0.0
()	%	81.5	71.5	67.5	42.5	38.1	40.1
CSI	Critical Success Index	0.3	0.3	0.5	0.4	0.5	0.7
HK	Hanssen and Kuipers disc	0.3	0.0	0.1	0.3	0.2	0.4
Bias	Bias	0.9	0.8	0.7	0.9	0.8	0.7
ME	Mean error	-0.2	-0.2	-0.5	-0.4	-0.5	-0.9
MAE	Mean Absolute error	1.5	2.0	1.6	2.7	3.5	2.8

		12_hour_High Elevation			Daily_High Elevation		
Notation	Statistics	3B42RT	3B42-V7	CMORPH	3B42RT	3B42-V7	CMORPH
POD	Probability of Detection	0.6	0.7	0.9	0.9	0.9	1.0
FAR	False Alarm Ratio	0.0	0.0	0.0	0.0	0.0	0.0
()	%	19.1	18.7	19.7	69.4	60.0	72.9
CSI	Critical Success Index	0.6	0.7	0.9	0.9	0.9	1.0
HK	Hanssen and Kuipers disc	0.3	0.0	0.6	0.9	-0.1	1.0
Bias	Bias	0.9	0.8	0.7	0.9	1.3	0.7
ME	Mean error	-0.7	-0.9	-1.9	-1.5	-1.8	-3.7
MAE	Mean Absolute error	4.2	4.5	3.9	0.9	1.0	0.9